

Research Article

DOI: <http://dx.doi.org/10.22192/ijamr.2022.09.12.011>

Cloning, Amplified Expression, Functional Characterisation and Purification of a *Pseudomonas putida* NCS1 Family Transport Protein

Irshad Ahmad[†], Karl A. Hassan[‡], Peter J. F. Henderson and Simon G. Patching*

School of Biomedical Sciences, University of Leeds, Leeds, UK

[†]Institute of Basic Medical Sciences, Khyber Medical University, Peshawar, Pakistan

[‡]School of Environmental and Life Sciences, University of Newcastle, Callaghan, Australia

*Correspondence: Professor Simon G. Patching, Astbury Building, Faculty of Biological Sciences, University of Leeds, Leeds LS2 9JT, UK.

E-mail: s.g.patching@leeds.ac.uk, simonpatching@yahoo.co.uk

Orcid

Irshad Ahmad: <https://orcid.org/0000-0003-3801-9279>

Karl A. Hassan: <https://orcid.org/0000-0003-2031-9679>

Peter J.F. Henderson: <http://orcid.org/0000-0002-9187-0938>

Abstract

Keywords

Allantoin,
Cloning strategy,
Nucleobase cation
symporter,
Protein purification,
Substrate specificity

Nucleobase Cation Symporter-1 (NCS1) secondary transport proteins are widespread in bacteria, archaea, fungi and plants. In bacteria they function in salvage pathways for nucleobases, nucleosides, hydantoin and related compounds. Only four bacterial NCS1 proteins are experimentally characterised: Mhp1 (5-arylhydantoin), PucI (allantoin), CodB and VPA1242 (cytosine). We cloned gene *PP_4309* for *Pseudomonas putida* protein AAN69889 (510 residues) into plasmid pTTQ18 with concomitant introduction of a C-terminal hexahistidine-tag and achieved amplified expression in *Escherichia coli* BL21 (DE3). AAN69889 is predicted to contain twelve transmembrane-spanning α -helices with both N- and C-terminal ends in the cytoplasm and shares good sequence homology with PucI (33.8% identical plus 24.7% highly similar residues). In transport assays using radiolabelled compounds, AAN69889 mediated uptake of ¹⁴C-allantoin into energised whole cells and no significant uptake of any other compound. ¹⁴C-allantoin uptake was not sodium dependent, suggesting that AAN69889 is driven by a proton gradient. The concentration-dependence of ¹⁴C-allantoin uptake by

AAN69889 conformed to Michaelis-Menten kinetics producing values for the apparent affinity of substrate transport (K_m) and maximum velocity (V_{max}) of $39.2 \pm 2.7 \mu\text{M}$ and $14.8 \pm 0.3 \text{ nmol/mg cells/15 sec}$, respectively. Competition of ^{14}C -allantoin uptake by unlabelled compounds identified AAN69889 as highly specific for allantoin. Database information currently describing AAN69889 as a nucleoside transporter can be changed to allantoin transporter. AAN69889 was stable to detergent solubilisation and Ni-NTA purification, achieving a purity of ~80% and a yield of ~1.2 mg/litre from fermentor cultures, and it had stable α -helical content. All making it tractable to further structural and biophysical characterisation.

1. Introduction

The Nucleobase Cation Symporter-1 (NCS1) family of secondary active transport proteins are widespread in Gram-negative and Gram-positive bacteria, archaea, fungi and plants (de Koning and Diallinas, 2000; Pantazopoulou and Diallinas, 2007; Saier et al., 2009; Weyand et al., 2010; Witz et al., 2014; Kryptou et al., 2015; Ma et al., 2016; Sioupouli et al., 2017; Patching, 2018). These proteins generally function in salvage pathways as transporters for purine and pyrimidine nucleobases and nucleosides, hydantoin and other related compounds including pyridoxine, thiamine and uric acid. NCS1 proteins are usually 419-635 amino acid residues in length, predicted to possess twelve transmembrane spanning α -helices (Saier et al., 2009; Witz et al., 2014) and function using a symport mechanism driven by a proton or sodium gradient (Kryptou et al., 2015). The common transport mechanism catalysed by NCS1 proteins is simplified as: Nucleobase or Hydantoin or Vitamin (out) + H^+ or Na^+ (out) Nucleobase or Hydantoin or Vitamin (in) + H^+ or Na^+ (in). NCS1 proteins show no sequence similarity to the NCS2 family, also known as the Nucleobase Ascorbate Transporter (NAT) family (Goudela et al., 2005; Diallinas and Gournas, 2008; Gournas et al., 2008; Frillingos, 2012). The first structural model for the NCS1 family was the sodium-coupled hydantoin transport protein, Mhp1, from *Microbacterium liquefaciens* (Suzuki and Henderson, 2006; Jackson et al., 2013), for which crystal structures have been determined with the protein in three different conformations i.e. outward-facing open, occluded with substrate and inward-facing open (Weyand et al., 2008; Shimamura et al., 2010; Simmons et al., 2014).

Mhp1 has provided a principal model for the alternating access mechanism of membrane transport and for the mechanism of ion-coupling (Shimamura et al., 2010; Adelman et al., 2011; Weyand et al., 2011; Shi, 2013; Kazmier et al., 2014; Kazmier et al., 2016). The function and substrate specificities of only 25 NCS1 proteins (4 bacterial, 16 fungal, 6 plant) have so far been characterised experimentally (Schwacke et al., 2003; Kryptou et al., 2015; Patching, 2018). The three other characterised bacterial NCS1 proteins are allantoin transporter PucI from *Bacillus subtilis* (Ma et al., 2016) and cytosine transporters CodB from *Escherichia coli* (Danielsen et al., 1995) and VPA1242 from *Vibrio parahaemolyticus* (Ahmad et al., 2020). The fungal proteins are Fur-type transporters FurA (allantoin), FurD (uracil, uric acid), FurE (uracil, uric acid, allantoin), Fur4 (uracil), Dal4 (allantoin), Fui1 (uridine) and the Fcy-type transporters FcyA - FcyE (purines, cytosine), Fcy2 (purines, cytosine), Thi7 (thiamine), Tpn1 (pyridoxine), Nrt1 (nicotinamide riboside) from *Aspergillus nidulans* and *Saccharomyces cerevisiae* (Hamari et al., 2009; Kryptou et al., 2015; Sioupouli et al., 2017). The plant transporters are AtNCS1 (PLUTO) from *Arabidopsis thaliana* (adenine, guanine, uracil) (Mourad et al., 2012; Witz et al., 2014), CtNCS1 from *Chlamydomonas reinhardtii* (adenine, guanine, uracil, allantoin) (Schein et al., 2013), ZmNCS1 from *Zea mays* (adenine, guanine, cytosine), SvNCS1 from *Setaria viridis* (adenine, guanine, hypoxanthine, cytosine, allantoin) (Rapp et al., 2016) and PpNCS1A and PpNCS1B from *Physcomitrella patens* (uracil, guanine, 8-azaguanine, 8-azaadenine, cytosine, 5-fluorocytosine, hypoxanthine, xanthine) (Minton et al., 2016).

Studies suggest that the two distinct fungal NCS1 subfamilies and the plant homologues originated through independent horizontal transfers from prokaryotes and demonstrate that transport activities in NCS1 proteins appeared independently by convergent evolution (Kryptou et al., 2015; Sioupouli et al., 2017). This is one explanation for the observation that substrate specificities of (fungal and plant) NCS1 proteins cannot be predicted by simple amino acid sequence comparisons, by phylogenetic analyses or from comparisons of amino acid residues in the major substrate binding site. Indeed, comparisons performed with Fur-type and Fcy-type NCS1 fungal transporters showed how identical or highly similar residues can provide different substrate specificities due to convergent evolution within the major substrate binding site (Kryptou et al., 2015; Sioupouli et al., 2017). Further investigations into the origins of substrate specificity in the wider NCS1 family are therefore warranted, especially those from bacteria. In this work we present results for cloning, amplified expression, functional characterisation and purification of NCS1 transport protein AAN69889 from *Pseudomonas putida* (UniProt entry Q88EZ1).

The opportunistic Gram-negative bacterium *P. putida* is the paradigm for a subclass of proteobacteria found widespread in terrestrial and aquatic environments (Palleroni, 1984). The important metabolic activities of these bacteria include element cycling and degradation of biogenic and xenobiotic pollutants (Timmis, 2002). *Pseudomonas* species have great potential for biotechnological applications, especially in areas of bioremediation (Dejonghe et al., 2001), biocatalysis (Schmid et al., 2001), as biocontrol agents in plant protection (Walsh et al., 2001) and for production of novel bioplastics (Kahlon, 2016). *P. putida* strain KT2440 is the best characterised *pseudomonas* species and was the first Gram-negative soil bacterium to be certified as a safety strain by the Recombinant DNA Advisory Committee (Federal Register, 1982). It has been estimated that *P. putida* strain KT2440 possesses 350 cytoplasmic membrane transport

systems, five of which are classed as belonging to the NCS1 family (Nelson et al., 2008).

For investigating *P. putida* protein AAN69889, we used a well-established strategy for cloning bacterial transport proteins with a C-terminal hexahistidine tag in *Escherichia coli* using plasmid pTTQ18, followed by optimisation of conditions for amplified expression. The functional activity of AAN69889-His₆ was characterized in terms of substrate and ion specificity, transport kinetics, and ligand recognition. AAN69889-His₆ was purified by immobilised metal affinity chromatography (IMAC) with a Ni-NTA resin, followed by analysis of secondary structure integrity and thermal stability using circular dichroism spectroscopy and ligand binding activity by fluorescence spectroscopy.

2. Materials and Methods

2.1. General

For details of general materials, sources, methods and equipment see the Supplementary Information.

2.2. Cloning and amplified expression

Cloning and amplification of expression of *P. putida* protein AAN69889 in *E. coli* was achieved using a strategy that we and others have found successful with a wide range of bacterial and archaeal membrane proteins (Ward et al., 1999; Saidijam et al., 2003; Saidijam et al., 2005; Clough et al., 2006; Suzuki and Henderson, 2006; Szakonyi et al., 2007; Gordon et al., 2008; Ma et al., 2008; Bettaney et al., 2013; Ma et al., 2013; Ma et al., 2016). This involved design of PCR primers (Forward: 5'-CCGGAATTCGCATATGAGTAGCAGCCTCGACCTTGCCCCTG-3'; Reverse: 5'-AAAACCTGCAGCATGGCCGCTGTGGTTCGACGGCGATGCAC-3') to extract and amplify the specific gene from genomic DNA of *P. putida* KT2440, introducing *EcoRI* and *PstI* restriction sites at the 5' and 3' ends, respectively. The restriction-

digested PCR product was ligated into plasmid pTTQ18 (Stark, 1987) immediately upstream from a hexahistidine (His₆) tag coding sequence and the resultant pTTQ18-gene(His₆) construct was used to transform *E. coli* BL21(DE3) cells. For full details of the cloning procedure see Supplementary Methods. Expression tests were initially performed using small scale cultures (50 ml) in LB medium supplemented with carbencillin (100 µg/ml), induction with IPTG (0.5 mM) at A₆₀₀ = 0.6 and then growth for a further 2 hours. Total (inner plus outer) membranes from induced and uninduced cells were isolated using the water lysis procedure (Witholt et al., 1976; Ward et al., 2000) and analysed by SDS-PAGE and Western blotting using an antibody to the His₆ epitope for detection of amplified protein bands. Conditions for optimising the amplified expression level of AAN69889-His₆ were tested by using ranges in the concentration of IPTG for induction (0-1 mM) and the length of induction (2-5 hours) and using three different types of media for cell growth (LB, 2TY, M9 minimal). To provide enough protein for purification and further analysis, optimised culture conditions were scaled up to volumes of 10 litres in flasks or 30 litres in a fermentor, and the resultant cells used for isolation of inner membranes by sucrose density gradient ultracentrifugation. For full details of cell growth and membrane preparation procedures see the Supplementary Information.

2.3. Whole cell transport and competition assays

Measurements of uptake of radiolabelled compounds into energised whole cells of *E. coli* were performed using a method based on that of Henderson et al., (1977). ¹⁴C-allantoin, ³H-L-5-benzylhydantoin and ¹⁴C-L-5-indolylmethylhydantoin were synthesised in-house (Patching, 2009, Patching, 2011, Patching, 2017) and other radiolabelled compounds were from Perkin Elmer Ltd, UK. Cells were grown in LB medium supplemented with glycerol (20 mM) and carbencillin (100 µg/ml) in volumes of 50 or 100 ml at 37 °C in 250 ml or 500 ml baffled conical flasks with aeration at 220 rpm to an A₆₀₀

of ~0.8. The cells were then either left uninduced or induced with IPTG (0.2 mM) and grown for a further 1 hour. After harvesting by centrifugation (4,000 rpm, 10 min, in Falcon tubes using a bench-top instrument), the cells were washed three times with 40 ml transport buffer (150 mM KCl, 5 mM MES, pH 6.6) and then resuspended in the same buffer to an A₆₈₀ of 2.0. The basic method for the assay is described as follows. Cells were energised for building up the proton gradient to drive substrate transport by incubating aliquots of the suspension (955 µl) with 20 mM glycerol (20 µl of 1 M) and with bubbled air in a bijou bottle held in a water jacket at 25 °C. After exactly 3 minutes, radiolabelled substrate at a concentration of 50 µM (25 µl of a 2 mM stock solution) was added with brief mixing. At time points of 0.25, 1, 2, 5, 7.5 and 10 minutes after adding the radiolabelled substrate, 100 µl aliquots were transferred to cellulose nitrate filters (0.45 µm pore size), pre-soaked in transport buffer, on a vacuum manifold and washed immediately with transport buffer (3 ml) three times. The filters were transferred to scintillation vials with 10 ml Emulsifier Safe liquid scintillation fluid (Perkin Elmer Ltd, UK) and incubated overnight. The level of radioactivity retained by the cells was measured by liquid scintillation counting (Packard Tri-Carb 2100TR instrument). Background counts were measured from washing filters under vacuum in the absence of cells or radiolabelled substrate. Standard counts were measured by transferring 4 µl of the radiolabelled substrate stock solution (containing 8 nmol) directly to a washed filter in the vial. The uptake of radiolabelled substrate into the cells was calculated using the following equation: Uptake (nmol/mg cells) = (Cell counts – Background counts) x (Total assay volume/Sample taken volume) x (1/mg of cells) x (Moles of standard/Standard counts); where dry weight of cells (mg) = Total assay volume (ml) x A₆₈₀ x 0.68. The times of sampling and/or of added radiolabelled substrate concentration were varied for kinetic analyses. To test the effect of potential competing compounds on ¹⁴C-allantoin uptake the unlabelled compound was added from a stock solution (50 mM) in 100% DMSO to the cells prior to the energisation period, the final

concentration of the unlabelled compound was 500 μM and the final concentration of DMSO was 1%. Relative uptake values were measured as a percentage of those obtained from samples in the absence of any added unlabelled compound or DMSO.

2.4. Protein solubilisation and purification

Inner membranes were solubilised for up to 4 hours at 4 °C in solubilisation buffer (Supplementary Table S1). The membranes were then sedimented at 131,000 x g for 1 hour at 4 °C to remove the insoluble fraction. For purification by immobilised-metal affinity chromatography (IMAC), the supernatant was incubated with Ni-NTA resin for 2 hours at 4 °C with mixing and then transferred to a BioRad column and the supernatant was run through the column to elute unbound components. The resin was washed with 150-200 ml of wash buffer 1 (Supplementary Table S1) to remove any remaining unbound material. The His₆-tagged protein was removed by addition of elution buffer (Supplementary Table S1). Volumes of eluted samples were reduced to 3 ml using Vivaspin 20 tube concentrators (4,000 xg) with molecular weight cut off (MWCO) 100 kDa. The 3 ml sample was then applied to a BioRadEcono-pac 10 DG desalting column to remove the high concentration of imidazole. When the sample had run into the column, 4.5 ml of wash buffer 2 (Supplementary Table S1) was applied and the eluted fraction was collected in a Vivaspin 6 tube (MWCO 100 kDa) and spun at 4,000 x g. Purified protein concentrated to 5-30 mg/ml was dispensed into aliquots, flash frozen in liquid nitrogen and stored at -80 °C.

2.5. Circular dichroism spectroscopy

The secondary structure content of purified AAN69889-His₆ was measured by far-UV circular dichroism (CD) spectroscopy using a CHIRASCAN instrument (Applied Photophysics, UK) at 20 °C with constant nitrogen flushing. Protein samples (0.15 mg/ml) in 10 mM NaPi (pH 7.5) buffer plus 0.05% DDM were analysed in a Hellma quartz cuvette with a 1.0 mm pathlength.

Measurements in the wavelength range 180-260 nm used a scan rate of 1 nm/second. A spectrum of buffer alone was subtracted from all sample spectra. Thermal stability was analysed by ramping the temperature from 5-90 °C and finally back to 5 °C, where each increment was held for 60 seconds before a measurement was made. Changes in secondary structure were monitored at 209 nm. Melting temperatures were estimated using Global Analysis CD software-3. CD ellipticity values were converted to mean residue ellipticity (MRE, $\text{deg.cm}^{-2}.\text{dmol}^{-1}$).

2.6. Fluorescence spectroscopy

Steady-state spectrofluorimetry measurements were performed on purified AAN69889-His₆ to analyse ligand binding using a method based on that described by Ward et al., (2000). This exploited the intrinsic fluorescence properties of protein tryptophan residues and a quench in its intensity caused by the binding of ligand. Purified AAN69889-His₆ (2.5 μM) in fluorescence buffer (1 ml) (Supplementary Table S2) was analyzed using a Photon Technology International spectrofluorimeter in the presence and absence of 15 mM NaCl and stirred at 18 °C. For ligands that were not soluble in 100% fluorescence buffer, a ligand stock solution in 100% DMSO was used, giving a final DMSO concentration of no more than 2% in the assay sample. Fluorescence was excited at the wavelength that is absorbed by tryptophan residues (295 nm) and emission monitored over the wavelength range that is emitted during fluorescence (310-360 nm). To allow direct comparisons between measurements, slit widths of 0.6 nm and a step time of 0.5 sec were used for all measurements. Titrations of ligand at a range of concentrations (0-2 mM) were performed by additions of appropriate stock solutions into the sample. Following each ligand addition, samples were mixed for 1.5 minutes before the fluorescence emission was monitored. Data were analyzed to obtain apparent binding affinities (K_d values) using the Michaelis-Menten analysis or nonlinear regression tool in GraphPad Prism 7 software.

3. Results and Discussion

3.1. Database and computational analysis of *P. putida* protein AAN69889

The function and substrate specificities of only 25 NCS1 proteins (3 bacterial, 16 fungal, 6 plant) have so far been characterised experimentally. The putative substrate specificities of other NCS1 proteins given in databases are therefore based on predictions only or may be based on gene locus positions with respect to other nearby genes, e.g. as part of a cluster of genes responsible for transport and metabolism of a specific solute. Various protein databases currently list *P. putida* protein AAN69889 as a nucleoside transporter, e.g.

UniProt (<http://www.uniprot.org/uniprot/Q88EZ1>).

According to the Pseudomonas Genome Database (<http://beta.pseudomonas.com/>) (Winsor et al., 2016), the gene that codes for protein AAN69889 (510 residues) is at a locus position (*PP_4309*) directly upstream from a gene (*PP_4310*) that codes for a hydantoin racemase. Based on separate sequence alignments with characterised

bacterial NCS1 family proteins, AAN69889 has closest homology (33.8% identical plus 24.7% highly similar residues) with allantoin transporter PucI (Ma et al., 2016) and shares fewer identical residues with Mhp1 and CodB (27.0% and 22.6%, respectively). These observations suggested that allantoin could be a substrate for AAN69889.

Analysis of the AAN69889 amino acid sequence using the prediction tools TMHMM (<http://www.cbs.dtu.dk/services/TMHMM/>) (Krogh et al., 2001) and TOPCONS (<http://topcons.cbr.su.se/>) (Bernsel et al., 2009) suggested that the protein contains eleven or twelve transmembrane-spanning α -helices, respectively (Figure S1). Based on structurally characterised NCS1 family proteins and a demonstrated reliability for TOPCONS (Hennerdal and Elofsson 2011; Tsirigos et al., 2015., Saidijam et al., 2018), twelve transmembrane helices is most likely to be correct. In this case, both the N- and C-terminal ends of the protein are predicted to reside at the cytoplasmic side of the membrane (Figure 1).

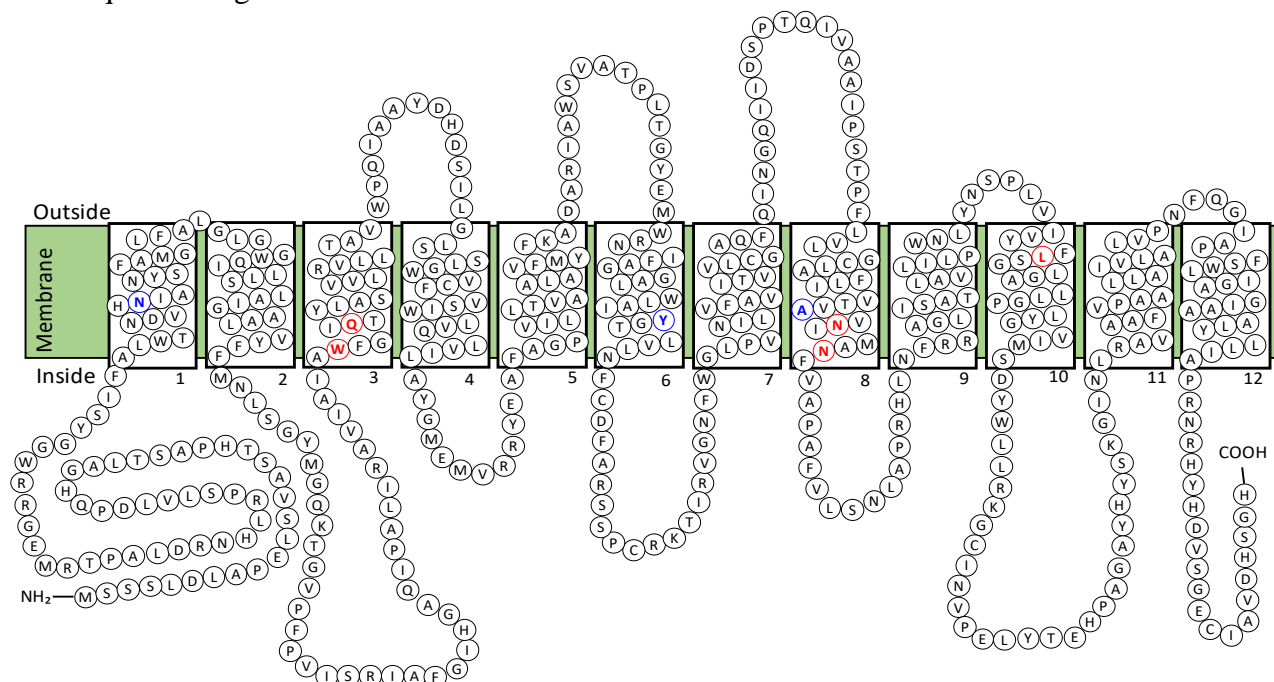


Figure 1. Predicted membrane topology of *P. putida* transport protein AAN69889. Diagram for the putative membrane topology of the AAN69889 transport protein of *P. putida* based on TOPCONS prediction for transmembrane helices (Figure S1). Twelve transmembrane-spanning α -helices are predicted and residues are coloured to show those that are identical (red) or highly similar (blue) compared with corresponding positions in the sodium and substrate binding site of Mhp1.

3.2. Cloning and amplified expression of *P. putida* protein AAN6989 in *E. coli*

P. putida protein AAN69889 was tractable to an established strategy for amplified expression in *E. coli* of bacterial NCS1 family proteins using plasmid pTTQ18 with concomitant introduction of a C-terminal His₆ tag to assist protein purification (Ward et al., 1999; Saidijam et al., 2003; Saidijam et al., 2005; Clough et al., 2006; Suzuki and Henderson, 2006; Szakonyi et al., 2007; Gordon et al., 2008; Ma et al., 2008; Bettaney et al., 2013; Ma et al., 2013; Ma et al., 2016). Criteria included availability of genomic DNA for the organism of origin, absence of internal *EcoRI* and *PstI* restriction sites in the gene for the protein of interest, a predicted cytoplasmic location of the protein C-terminus and availability of radiolabelled potential substrates for transport activity assays.

The gene *PP_4309* from *P. putida* KT2440 that encodes AAN69889 was successfully amplified by PCR (Figure S2A) and ligated into plasmid pTTQ18, as confirmed by restriction digestion analysis (Figure S2B) and DNA sequencing. The plasmid construct was transformed into *E. coli* strain BL21(DE3) and small-scale growth in LB medium showed amplified expression of AAN69889-His₆ based on detection of protein bands by SDS-PAGE and Western blotting against the C-terminal His₆ epitope (Figure 2). Based on various parameters that can be altered for improving the level of recombinant protein expression (Ahmad et al., 2018), growth and induction conditions for amplifying expression of AAN69889-His₆ in *E. coli* BL21(DE3) were optimised and found to be LB medium supplemented with 20 mM glycerol, induction with 0.25 mM IPTG and a post-induction period of 3 hours (Figure S3 and Figure S4).

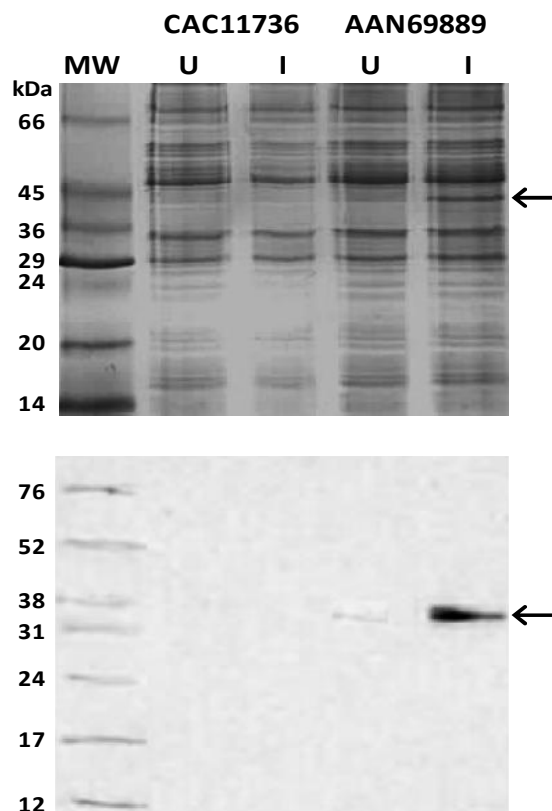


Figure 2. Test for amplified expression of *P. putida* protein AAN69889 in *E. coli*. Coomassie-stained SDS-PAGE (top) and Western blot (bottom) analyses of total membrane preparations from *E. coli* BL21(DE3) cells containing pTTQ18-derived plasmids for amplifying expression of *P. putida* protein AAN69889-His₆ alongside *Thermoplasma acidophilum* protein CAC11736-His₆ (as negative comparison) from cultures in LB medium that were left uninduced (U) or induced with 0.5 mM IPTG for 2 hours (I). MW = molecular weight markers. The arrow indicates the position of AAN69889-His₆.

In these tests it was observed that all cultures induced with IPTG in the range 0.1-1.0 mM showed a marginal decrease in growth rate after induction compared with cells that were left uninduced (Figure S3A), indicating that overexpression was happening. Following an induction period of 2 hours, all induced cultures reached an A_{680} of around 2.4. It can be noted that the protein would still express in uninduced cells and this leaky expression is characteristic of the operator-promoter system in plasmid pTTQ18 (Stark, 1987). Cultures using LB medium achieved the highest cell density ($A_{680} = \sim 3.2$), whilst cultures using 2TY medium reached a slightly lower cell density ($A_{680} = \sim 2.9$) and those using M9 minimal medium reached to a significantly lower cell density ($A_{680} = \sim 1.8$) (Figure S4). In each respective medium, cell growth in induced cells was marginally lower than in uninduced cells, which is indicative of protein overexpression.

3.3. Substrate and ion specificities of *P. putida* protein AAN69889

Initial time-dependence measurements for uptake of radiolabelled potential NCS1 substrates (50 μM) into energised *E. coli* cells induced for amplified expression of AAN69889 suggested that AAN69889 is a transporter of allantoin (Figure S5). Uptake of ^{14}C -allantoin was significantly greater in induced cells compared with uninduced cells with values after 2 minutes of around 19.5 and 3.6 nmol mg^{-1} cells, respectively. None of the other compounds tested showed significant transport activity, including

nucleobases and nucleosides. Transport of ^{14}C -allantoin by AAN69889 was confirmed by comparing uptake into induced versus uninduced cells and also into cells containing plasmid pTTQ18 with no gene insert (Figure 3). There was some uptake into uninduced cells, which was attributed to leaky expression from the plasmid, and negligible uptake into cells containing pTTQ18. Transport of ^{14}C -allantoin by AAN69889 showed no dependence on sodium over the concentration range 0-150 mM, suggesting that the protein is driven by a proton gradient (Supplementary Figure S6). The concentration-dependence of ^{14}C -allantoin uptake (0-500 μM) into cells induced for AAN69889 expression conformed to Michaelis-Menten kinetics producing values for the apparent affinity of substrate transport (K_m) and maximum velocity (V_{max}) of $39.17 \pm 2.66 \mu\text{M}$ and $14.77 \pm 0.27 \text{ nmol/mg cells/15 sec}$, respectively. Uptake into uninduced cells also showed concentration-dependence, but this was negligible, producing K_m and V_{max} values of $20.56 \pm 4.32 \mu\text{M}$ and $0.51 \pm 0.02 \text{ nmol/mg cells/15 sec}$, respectively (Figure 4). Kinetic parameters for ^{14}C -allantoin uptake by AAN69889 were similar to those obtained for PucI, which produced typical K_m and V_{max} values of $24.4 \pm 3 \mu\text{M}$ and $14.8 \text{ nmol/mg cells/15 sec}$, respectively (Ma et al., 2016). These results confirm that allantoin is the main substrate of AAN69889, which was predicted based on closest evolutionary relationship with PucI. The results also demonstrate how it is important to perform experimental assessments of substrate specificity when characterising transport protein function and not to rely on database information/predictions.

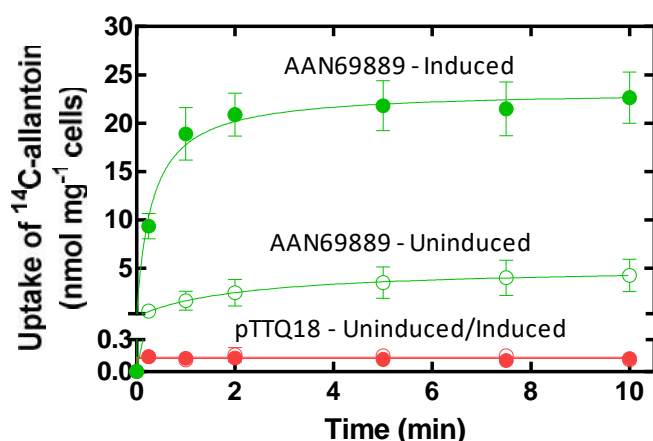


Figure 3. Confirmation of ^{14}C -allantoin transport by *P. putida* protein AAN69889. Uptake of ^{14}C -allantoin ($50\ \mu\text{M}$) into *E. coli* BL21(DE3) cells harbouring the plasmid pTTQ18/AAN69889 (green) or the empty plasmid pTTQ18/no gene (red) from cultures grown in LB medium supplemented with 20 mM glycerol and 100 $\mu\text{g}/\text{ml}$ of carbenicillin at 37 °C with shaking at 220 rpm. Cells were left uninduced (open circles) or were induced (closed circles) at $A_{680} = 0.6$ with IPTG (0.25 mM) and then grown for a further 1 hour. Harvested cells were washed three times using transport assay buffer (150 mM KCl, 5 mM MES pH 6.6) and resuspended in the same buffer to an accurate A_{680} of around 2.0. Cells were energised with glycerol (20 mM) and tested for uptake ^{14}C -allantoin at the given time points. Data points represent the average of duplicate measurements and the plots were produced using GraphPad Prism 7 software.

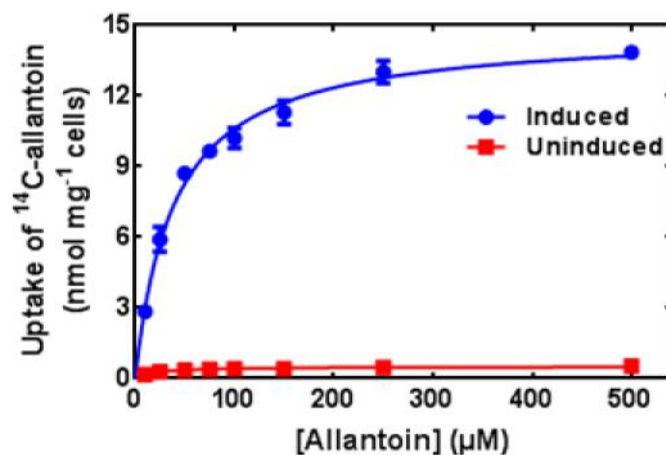


Figure 4. Concentration-dependence of ^{14}C -allantoin uptake by *P. putida* protein AAN69889. Uptake of ^{14}C -allantoin (0-500 μM) into *E. coli* BL21(DE3) cells harbouring the plasmid pTTQ18/AAN69889. Cells were grown in LB medium supplemented with 20 mM glycerol and 100 $\mu\text{g}/\text{ml}$ of carbenicillin at 37 °C with shaking at 220 rpm. Cells were left uninduced (red) or were induced (blue) at an $A_{680} = 0.6$ with IPTG (0.25 mM) and then grown for a further 1 hour. Harvested cells were washed three times using transport assay buffer (150 mM KCl, 5 mM MES pH 6.6) and resuspended in the same buffer to an accurate A_{680} of around 2.0. Cells were energised with glycerol (20 mM) and tested for uptake of the given concentrations of ^{14}C -allantoin 15 seconds post addition. Data points represent the average of duplicate measurements and the plots were produced using GraphPad Prism 7 software.

3.4. Ligand recognition by *P. putida* protein AAN69889

The specificity of ligand recognition by AAN69889 was tested through competition of ^{14}C -allantoin transport (50 μM) with a ten-fold excess of unlabelled NCS1 substrates and related compounds (500 μM) (Figure 5 and Figure S7). By far the greatest competitive effect was produced by allantoin, which reduced transport activity to 11.2% and 8.4% at time points of 15 seconds and 2 minutes, respectively. The next most effective competitors were the chemically similar uracil and hydantoin, which reduced

transport activity to 66.6/51.9% and 77.0/64.6% after 15 seconds and 2 minutes, respectively. It should be pointed out that addition of DMSO (1%) alone, which was used to dissolve some of the compounds, reduced transport activity to 76.3% and 85.1% at 15 seconds and 2 minutes, respectively. All other compounds produced transport activity values greater than 80% compared with non-competed cells. These results demonstrate a high specificity for allantoin recognition by AAN69889, which is more specific than the pattern of ligand recognition produced by PucI (Ma et al., 2016).

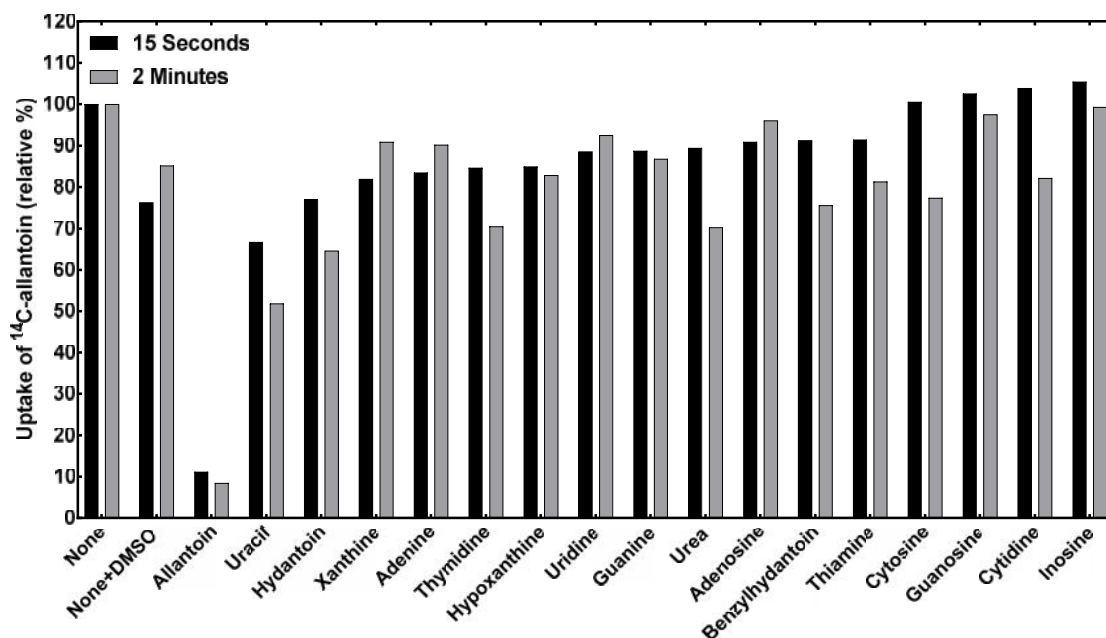


Figure 5. Ligand specificity of *P. putida* protein AAN69889. Competition of ^{14}C -allantoin (50 μM) uptake into *E. coli* BL21(DE3) cells expressing AAN69889-His₆ in the presence of a ten-fold molar excess of potential unlabelled competitors. The non-competed uptake rate was taken as 100% corresponding to 15 seconds and 2 minutes post-addition of ^{14}C -allantoin, respectively. All data represent the average of duplicate measurements. None = no competitors.

3.5. Conservation of residues for substrate specificity and ligand recognition in bacterial NCS1 family proteins

Following the results described here, the substrate specificities of four bacterial NCS1 proteins have now been characterised experimentally: Mhp1 (5-arylhydantoin), PucI (allantoin), AAN69889

(allantoin) and CodB (cytosine). Based on the nine residues involved in substrate binding in Mhp1, we can compare the residues at corresponding positions in the other proteins to look for possible explanations about the origin of substrate specificity in bacterial NCS1 proteins (Table 1, Figure 1 and Figure S8).

Two positions, corresponding to Mhp1 residues Trp117 in TMIII and Leu363 in TMX, are identically conserved in all four proteins. Two further positions, corresponding to Mhp1 residues Gln121 in TMIII and Asn318 in TMVIII, are identically conserved in PucI and in AAN69889. Residues at these four positions are all involved in direct interactions with the hydantoin ring of substrates bound to Mhp1 (Simmons et al., 2014) and therefore appear to be necessary for recognition of hydantoins. These observations also support the small but significant competitive effects of uracil and hydantoin on ¹⁴C-allantoin transport by AAN69889. Three positions, corresponding to Mhp1 residues Gln42 in TMI, Gly219 and Ala222 in TMVI, are not conserved in any other proteins, but these positions are identical in PucI and AAN69889. These three

positions, which are occupied by Asn, Ile and Thr in PucI and AAN69889, appear to explain the ability of the latter proteins to transport allantoin that is not possible by Mhp1. There are also two positions in PucI and AAN69889 that are not identical with each other, which correspond to Mhp1 residues Ala44 in TMI and Trp220 in TMVI. AAN69889 residue Ala67 is conserved with Mhp1 Ala44 and PucI residue Trp240 is conserved with Mhp1 residue Trp220. These differences reflect the fact that the overall sequence identity between PucI and AAN69889 is 33.8%. Caution should of course be declared about making possible structural explanations for differences in substrate specificity between NCS1 proteins, as demonstrated by studies on the fungal transporters (Kryptou et al., 2015; Sioupolou et al., 2017).

Table 1. Conservation of substrate binding residues in characterised bacterial NCS1 family proteins. Residues in the substrate binding site of crystallographically defined Mhp1 (5-arylhydantoins) are compared with those at the corresponding positions in PucI (allantoin), AAN (allantoin) and CodB (cytosine) based on sequence alignments (Figure S7). Residues are coloured to indicate those that are identically conserved (*red*) or highly similar (*blue*) compared with residues in Mhp1.

	Mhp1	PucI	AAN	CodB
TMI	Gln42	Asn43	Asn65	Phe33
	Ala44	Pro45	Ala67	Ala35
TMIII	Trp117	Trp119	Trp141	Trp108
	Gln121	Gln123	Gln145	Gly112
TMVI	Gly219	Ile239	Ile258	Ser203
	Trp220	Trp240	Tyr259	Phe204
	Ala222	Thr242	Thr261	Ser206
TMVIII	Asn318	Asn329	Asn348	Leu284
TMX	Leu363	Leu377	Leu396	Leu325

3.6. Detergent solubilisation and purification of *P. putida* protein AAN69889

To provide sufficient material for purification of AAN69889-His₆, optimised growth and induction conditions were scaled up to 30 litre cultures in a fermentor followed by isolation of inner membranes. AAN69889-His₆ was solubilised from inner membranes using the detergent DDM (1%) and then purified by IMAC using a Ni-NTA resin with imidazole at a concentration of 20 mM for incubation and washing steps and 200 mM for

elution (Figure 6). The relative amount of AAN69889-His₆ in the supernatant was similar to the level in inner membranes, indicating that the large majority of membrane proteins had been solubilised by DDM. Negligible AAN69889-His₆ in the unbound fraction suggested that most of the AAN69889 protein was bound to the resin. This resulted in a purity for AAN69889-His₆ of around 80% based on densitometric analysis of the Coomassie-stained gel and a purification yield of around 1.2 mg/litre of cell culture.

On SDS-PAGE gels and Western blots, two associated bands in the purified protein were visible, which may be due to an unfolding property for a small fraction of the protein (Figure 6).

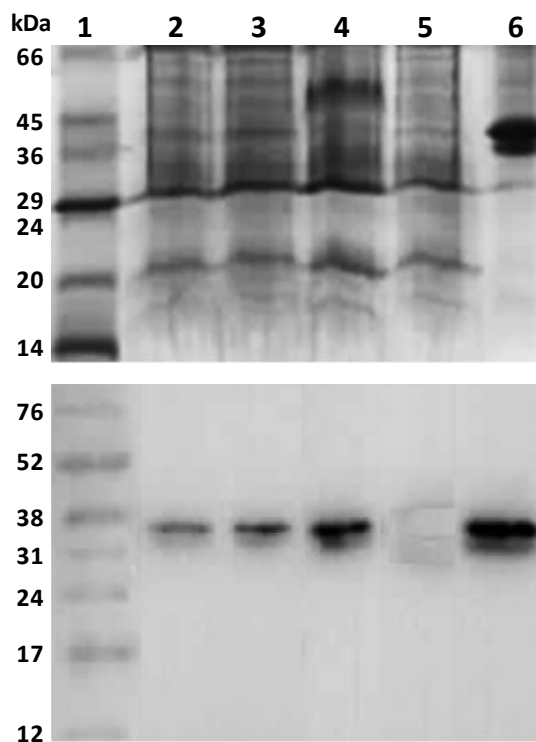


Figure 6. Solubilisation and purification of *P. putida* protein AAN69889 from inner membranes. Coomassie-stained SDS-PAGE (*top*) and Western blot (*bottom*) analyses for solubilisation (1% DDM) and IMAC purification of AAN69889-His₆ from inner membranes. Samples were loaded on the gel (16 µg) and blot (4 µg) as follows: 1 = molecular weight markers, 2 = inner membranes, 3 = supernatant (soluble fraction), 4 = membrane pellet (insoluble fraction), 5 = column flow-through (unbound fraction), 6 = eluted and concentrated protein.

Using the amino acid sequence of AAN69889-His₆, the protein has a theoretical mass of 56693.72 Da. In comparison, purified AAN69889-His₆ resolved by SDS-PAGE migrates at positions corresponding to molecular weights of 37 kDa and 38 kDa for the two protein bands (Figure S9). This size difference of ~68% is consistent with SDS-PAGE analysis of other NCS1 family proteins, which migrate at approximately 62-74% of their predicted sizes (Suzuki and Henderson, 2006; Bettaney et al., 2013; Ma et al., 2016). It is widely recognised that membrane proteins migrate anomalously on SDS-PAGE gels at lower molecular weight

positions than their actual molecular weights predicted from amino acid composition due to their hydrophobic nature, high binding of SDS or retention of secondary structure that facilitates migration through the gel (Ward et al., 2000; Rath et al., 2009; Rath and, Deber, 2013).

3.7. Secondary structure integrity and ligand binding activity of purified AAN69889-His₆

Purified AAN69889-His₆ had α -helix content according to far-UV circular dichroism spectroscopy (Figure 7), thus confirming secondary structure integrity of the DDM-solubilised protein.

A thermal ramping experiment produced a melting temperature of 46.2 °C and showed that the AAN69889-His₆ protein is reasonably stable for performing biophysical assays using a temperature range of 18-25 °C (Figure 7). Observation of allantoin binding to purified AAN69889-His₆ was attempted using steady-state spectrophotofluorimetry by exploiting the intrinsic fluorescence properties of protein tryptophan residues. A possible small binding effect was detected that was greater than the effect of DMSO alone (used to solubilise allantoin) and that conformed to Michaelis-Menten kinetics (Figure 8). The magnitude of the fluorescence quench at 332 nm was only up to around 3.2% at an allantoin concentration of 2 mM, which is relatively small compared with the

fluorescence quench of around 20% observed for *L*-benzylhydantoin binding to Mhp1 at the same concentration (Weyand et al., 2008; Simmons et al., 2016). It is possible that the substrate binding site in AAN69889 does not closely involve tryptophan, unlike the two tryptophan residues (Trp117 and Trp220) in the binding site of Mhp1. Furthermore, AAN69889 has a tyrosine residue at one of these positions (Tyr259), making it less sensitive for this type of assay. The possible small binding effect of allantoin to AAN69889-His₆ that was observed showed no sodium dependence, which is consistent with the transport activity experiments on AAN69889-His₆ and with similar experiments on allantoin transporter PucI (Ma et al., 2016).

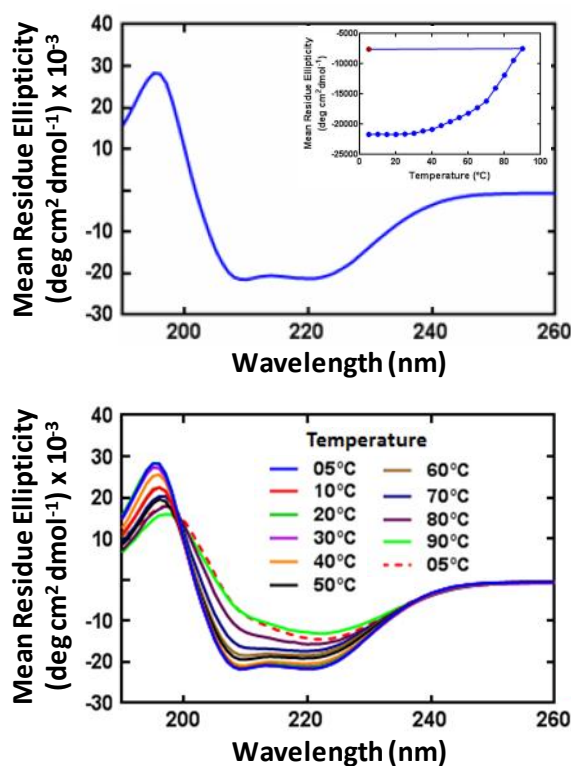


Figure 7. Secondary structure integrity of purified AAN69889-His₆. Far-UV (180-260 nm) circular dichroism spectrum for purified AAN69889-His₆ acquired using a CHIRASCAN instrument (Applied Photophysics, UK) at 20 °C with constant nitrogen flushing (*top*). The sample was prepared in a Hellma quartz cuvette of 1.0 mm pathlength at a final protein concentration of 0.15 mg/ml in CD buffer (10 mM NaPi pH 7.5, 0.05% DDM). Inset is a thermal unfolding profile over the temperature range 5-90 °C and finally back to 5 °C monitored at a wavelength of 209 nm. Full spectra from the thermal unfolding experiment are also shown (*bottom*).

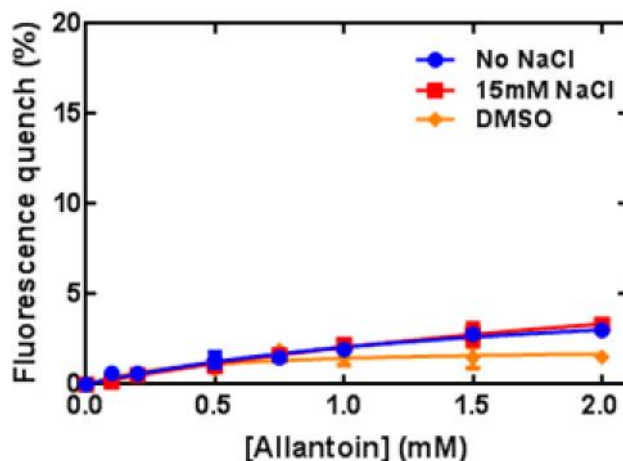


Figure 8. Possible detection of allantoin binding to *P. putida* protein AAN69889 by quenching of intrinsic fluorescence. Steady-state spectrophotofluorimetry measurements for detecting allantoin binding to purified AAN69889-His₆. Samples containing protein (2.5 μM) in fluorescence buffer (Supplementary Table S2) at 18 °C were excited at 295 nm and fluorescence emission was measured at 332 nm. Protein was pre-equilibrated with stirring for 1.5 minutes and then following additions of allantoin or DMSO, samples were stirred for 0.5 minutes before making the measurements. Data points represent the mean of triplicate measurements and error bars represent the standard deviations of the means. Data were fitted to the Michaelis-Menten equation in GraphPad Prism 7 software.

4. Conclusion

In this study, the gene for *P. putida* protein AAN69889 was successfully cloned into plasmid pTTQ18 and conditions for amplified expression of AAN69889-His₆ in *E. coli* were optimised. Allantoin was confirmed as the main, and possibly only, substrate of AAN69889. The protein was tractable to large scale production, detergent solubilisation and purification. A good purification yield, secondary structure integrity and stability of AAN69889-His₆ make it a promising candidate for crystallisation trials and for study of structure, ligand binding and dynamics using further biochemical and biophysical techniques. Mutagenesis studies should help us to better understand the origins of substrate specificity in AAN69889 and in other bacterial NCS1 proteins.

Acknowledgments

This work was supported by the University of Leeds. The authors thank Mr David Sharples (University of Leeds) for performing bacterial growths in a fermentor.

Conflict of interest

The authors declare that they have no conflict of interest.

References

- Adelman, J.L., Dale, A.L., Zwier, M.C., Bhatt, D., Chong L.T., Zuckerman, D.M. and Grabe, M. 2011. Simulations of the alternating access mechanism of the sodium symporter Mhp1. *Biophys. J.* 101(10): 2399–2407.
- Ahmad, I., Ma, P., Nawaz, N., Sharples, D.J., Henderson, P.J.F. and Patching, S.G. 2020. Cloning, amplified expression, functional characterisation and purification of *Vibrio parahaemolyticus* NCS1 cytosine transporter VPA1242 (Chapter 8). In: Patching SG (ed) *A Closer Look at Membrane Proteins*. Independent Publishing Network, UK, pp. 241-267. ISBN: 978-1-83853-535-3.

- Ahmad, I., Nawaz, N., Darwesh, N.M., ur Rahman, S., Mustafa, M.Z., Khan, S.B. and Patching, S.G. 2018. Overcoming challenges for amplified expression of recombinant proteins using *Escherichia coli*. Prot. Expr. Purif. 144: 12–18.
- Bernsel, A., Viklund, H., Hennerdal, A. and Elofsson, A. 2009. TOPCONS: consensus prediction of membrane protein topology. Nucleic Acids Res. 37(Web Server issue): W465–W468.
- Bettaney, K.E., Sukumar, P., Hussain, R., Siligardi, G., Henderson, P.J. and Patching, S.G. 2013. A systematic approach to the amplified expression, functional characterization and purification of inositol transporters from *Bacillus subtilis*. Mol. Membr. Biol. 30(1): 3–14.
- Clough, J., Saidijam, M., Bettaney, K.E., Szakonyi, G., Patching, S.G., Mueller, J., Shibayama, K., Bacon, M., Barksby, E., Groves, M., Herbert, R.B., Phillips-Jones, M.K., Ward, A., Gunn-Moore, F.J., O'Reilly, J., Rutherford, N.G., Bill, R. and Henderson, P.J.F. 2006. Prokaryotic membrane transport proteins: amplified expression and purification. In: Lundstrom KH (ed) Structural genomics on membrane proteins. Taylor and Francis, pp 21-42.
- Danielsen, S., Boyd, D. and Neuhard, J. 1995. Membrane topology analysis of the *Escherichia coli* cytosine permease. Microbiology 141(11): 2905–2913.
- Dejonghe, W., Boon, N., Seghers, D., Top, E.M. and Verstraete, W. 2001. Bioaugmentation of soils by increasing microbial richness: missing links. Env. Microbiol. 3(10): 649–657.
- de Koning, H. and Diallinas, G. 2000. Nucleobase transporters (review). Mol. Membr. Biol. 17(2): 75–94.
- Diallinas, G. and Gournas, C. 2008. Structure-function relationships in the nucleobase-ascorbate transporter (NAT) family: lessons from model microbial genetic systems. Channels (Austin) 2(5): 363–372.
- Federal Register. Certified host-vector systems. Washington, DC.1982; 47: 17197.
- Frillingos, S. 2012. Insights to the evolution of Nucleobase-Ascorbate Transporters (NAT/NCS2 family) from the Cys-scanning analysis of xanthine permease XanQ. Int J Biochem. Mol. Biol. 3(3): 250–272.
- Gordon, E., Horsefield, R., Swarts, H.G., de Pont, J.J., Neutze, R. and Snijder, A. 2008. Effective high-throughput overproduction of membrane proteins in *Escherichia coli*. Protein Expr. Purif. 62(1): 1–8.
- Goudela, S., Karatza, P., Koukaki, M., Frillingos, S. and Diallinas, G. 2005. Comparative substrate recognition by bacterial and fungal purine transporters of the NAT/NCS2 family. Mol. Membr. Biol. 22(3): 263–275.
- Gournas, C., Papageorgiou, I. and Diallinas, G. 2008. The nucleobase-ascorbate transporter (NAT) family: genomics, evolution, structure-function relationships and physiological role. Mol. Biosyst. 4(5): 404–416.
- Hamari, Z., Amillis, S., Drevet, C., Apostolaki, A., Vágvölgyi, C., Diallinas, G. and Scazzocchio, C. 2009. Convergent evolution and orphan genes in the Fur4p-like family and characterization of a general nucleoside transporter in *Aspergillus nidulans*. Mol. Microbiol. 73 (1): 43–57.
- Henderson, P.J., Giddens, R.A. and Jones-Mortimer, M.C. 1977. Transport of galactose, glucose and their molecular analogues by *Escherichia coli* K12. Biochem. J. 162(2): 309–320.
- Hennerdal, A. and Elofsson, A. 2011. Rapid membrane protein topology prediction. Bioinformatics 27(9): 1322–1323.
- Jackson, S.M., Patching, S.G., Ivanova, E., Simmons, K.J., Weyand, S., Shimamura, T., Brückner, F., Suzuki, S., Iwata, S., Sharples, D.J., Baldwin, S.A., Sansom, M.P.S., Beckstein, O., Cameron, A.D.,

- and Henderson, P.J.F. 2013. Mhp1, the Na(+)-hydantoin membrane transport protein. In: Roberts GCK (ed) Encyclopedia of Biophysics. Springer, pp 1514-1521.
- Kahlon, R.S. 2016. Pseudomonas: Molecular and Applied Biology. Springer, Switzerland. DOI: 10.1007/978-3-319-31198-2.
- Kazmier, K., Claxton, D.P. and Mchaourab, H.S. 2016. Alternating access mechanisms of LeuT-fold transporters: trailblazing towards the promised energy landscapes. Curr. Opin. Struct. Biol. 45: 100–108.
- Kazmier, K., Sharma, S., Islam, S.M., Roux, B. and Mchaourab, H.S. 2014. Conformational cycle and ion-coupling mechanism of the Na⁺/hydantoin transporter Mhp1. Proc. Natl. Acad. Sci. U. S. A. 111(41): 14752–14757.
- Krogh, A., Larsson, B., von Heijne, G. and Sonnhammer, E.L. 2001. Predicting transmembrane protein topology with a hidden Markov model: application to complete genomes. J. Mol. Biol. 305(3): 567–580.
- Kryptou, E., Evangelidis, T., Bobonis, J., Pittis, A.A., Gabaldón, T., Scazzocchio, C., Mikros, E. and Diallinas, G. 2015. Origin, diversification and substrate specificity in the family of NCS1/FUR transporters. Mol. Microbiol. 96(5): 927–950.
- Ma, P., Patching, S.G., Ivanova, E., Baldwin, J.M., Sharples, D., Baldwin, S.A. and Henderson, P.J. 2016. Allantoin transport protein, PucI, from *Bacillus subtilis*: evolutionary relationships, amplified expression, activity and specificity. Microbiology 162(5): 823–836.
- Ma, P., Varela, F., Magoch, M., Silva, A.R., Rosario, A.L., Oliveira, T.F., Oliveira, T.F., Nogly, P., Pessanha, M., Stelter, M., Kletzin, A., Henderson, P.J. and Archer, M. 2013. An efficient strategy for small-scale screening and production of archaeal membrane transport proteins in *Escherichia coli*. PLoS One 8(10): e76913.
- Ma, P., Yuille, H.M., Blessie, V., Göhring, N., Iglói, Z., Nishiguchi, K., Nakayama, J., Henderson, P.J. and Phillips-Jones, M.K. 2008. Expression, purification and activities of the entire family of intact membrane sensor kinases from *Enterococcus faecalis*. Mol. Membr. Biol. 25(6-7): 449–473.
- Minton, J.A., Rapp, M., Stoffer, A.J., Schultes, N.P. and Mourad, G.S. 2016. Heterologous complementation studies reveal the solute transport profiles of a two-member nucleobase cation symporter 1 (NCS1) family in *Physcomitrella patens*. Plant Physiol. Biochem. 100: 12–17.
- Mourad, G.S., Tippmann-Crosby, J., Hunt, K.A., Gicheru, Y., Bade, K., Mansfield, T.A. and Schultes, N.P. 2012. Genetic and molecular characterization reveals a unique nucleobase cation symporter 1 in Arabidopsis. FEBS Lett. 586(9): 1370–1378.
- Nelson, D.L., Lehninger, A.L. and Cox, M.M. 2008. Lehninger principles of biochemistry. New York: W.H. Freeman.
- Palleroni, N.J. 1984. Pseudomonas. In: Krieg, N.R., Holt, J.G. (eds) Bergey's Manual of Systematic Bacteriology. Williams & Wilkins, Baltimore MD, pp 1441-1499.
- Pantazopoulou, A. and Diallinas, G. 2007. Fungal nucleobase transporters. FEMS Microbiol. Rev 31(6): 657–675.
- Patching, S.G. 2009. Synthesis of highly pure ¹⁴C-labelled DL-allantoin and ¹³C NMR analysis of labelling integrity. J. Labelled Compd. Radiopharm. 52(9): 401–404.
- Patching, S.G. 2011. Efficient syntheses of ¹³C- and ¹⁴C-labelled 5-benzyl and 5-indolylmethyl L-hydantoins. J. Label. Compd. Radiopharm. 54(2): 110–114.
- Patching, S.G. 2017. Synthesis, NMR analysis and applications of isotope-labelled hydantoins. Journal of Diagnostic Imaging in Therapy 4(1): 3–26.

- Patching, S.G. 2018. Recent developments in Nucleobase Cation Symporter-1 (NCS1) family transport proteins from bacteria, archaea, fungi and plants. *J. Biosci.* 43(4): 797–815.
- Rapp, M., Schein, J., Hunt, K.A., Nalam, V., Mourad, G.S. and Schultes, N.P. 2016. The solute specificity profiles of nucleobase cation symporter 1 (NCS1) from *Zea mays* and *Setaria viridis* illustrate functional flexibility. *Protoplasma* 253(2): 611–623.
- Rath, A. and Deber, C.M. 2013. Correction factors for membrane protein molecular weight readouts on sodium dodecyl sulfate-polyacrylamide gel electrophoresis. *Anal. Biochem.* 434(1): 67-72.
- Rath, A., Glibowicka, M., Nadeau, V.G., Chen, G. and Deber, C.M. 2009. Detergent binding explains anomalous SDS-PAGE migration of membrane proteins. *Proc. Natl. Acad. Sci. U. S. A.* 106(6): 1760–1765.
- Saidijam, M., Azizpour, S. and Patching, S.G. 2018. Comprehensive analysis of the numbers, lengths and amino acid compositions of transmembrane helices in prokaryotic, eukaryotic and viral integral membrane proteins of high-resolution structure. *J. Biomol. Struct. Dyn.* 36(2): 443–464.
- Saidijam, M., Bettaney, K.E., Szakonyi, G., Psakis, G., Shibayama, K., Suzuki, S., Clough, J.L., Blessie, V., Abu-Bakr, A., Baumberg, S., Mueller, J., Hoyle, C.K., Palmer, S.L., Butaye, P., Walravens, K., Patching, S.G., O'Reilly, J., Rutherford, N.G., Bill, R.M., Roper, D.I., Phillips-Jones, M.K. and Henderson, P.J. 2005. Active membrane transport and receptor proteins from bacteria. *Biochem. Soc. Trans.* 33(4): 867–872.
- Saidijam, M., Psakis, G., Clough, J.L., Mueller, J., Suzuki, S., Hoyle, C.J., Palmer, S.L., Morrison, S.M., Pos, M.K., Essenberg, R.C., Maiden, M.C., Abu-bakr, A., Baumberg, S.G., Neyfakh, A.A., Griffith, J.K., Stark, M.J., Ward, A., O'Reilly, J., Rutherford, N.G., Phillips-Jones, M.K. and Henderson, P.J. 2003. Collection and characterisation of bacterial membrane proteins. *FEBS Lett.* 555(1): 170–175.
- Saier, M.H. Jr, Yen, M.R., Noto, K., Tamang, D.G. and Elkan, C. 2009. The Transporter Classification Database: recent advances. *Nucleic Acids Res.* 37(Database issue): D274–D278.
- Schein, J.R., Hunt, K.A., Minton, J.A., Schultes, N.P. and Mourad, G.S. 2013. The nucleobase cation symporter 1 of *Chlamydomonas reinhardtii* and that of the evolutionarily distant *Arabidopsis thaliana* display parallel function and establish a plant-specific solute transport profile. *Plant Physiol. Biochem.* 70: 52–60.
- Schmid, A., Dordick, J., Hauer, B., Kiener, A., Wubbolts, M. and Witholt, B. 2001. Industrial biocatalysis today and tomorrow. *Nature* 409: 258–268.
- Schwacke, R., Schneider, A., van der Graaff, E., Fischer, K., Catoni, E., Desimone, M., Frommer, W.B., Flügge, U.I. and Kunze, R. 2003. ARAMEMNON, a novel database for *Arabidopsis* integral membrane proteins. *Plant. Physiol.* 131(1): 16–26.
- Shi, Y. 2013. Common folds and transport mechanisms of secondary active transporters. *Annu. Rev. Biophys.* 42: 51–72.
- Shimamura, T., Weyand, S., Beckstein, O., Rutherford, N.G., Hadden, J.M., Sharples, D., Sansom, M.S., Iwata, S., Henderson, P.J. and Cameron, A.D. 2010. Molecular basis of alternating access membrane transport by the sodium-hydantoin transporter Mhp1. *Science* 328(5977): 470–473.
- Simmons, K.J., Jackson, S.M., Brueckner, F., Patching, S.G., Beckstein, O., Ivanova, E., Geng, T., Weyand, S., Drew, D., Lanigan, J., Sharples, D.J., Sansom, M.S., Iwata, S., Fishwick, C.W., Johnson, A.P., Cameron, A.D. and Henderson, P.J. 2014. Molecular

- mechanism of ligand recognition by membrane transport protein, Mhp1. *EMBO J.* 33(16): 1831–1844.
- Sioupouli, G., Lambrinidis, G., Mikros, E., Amillis, S. and Diallinas, G. 2017. Cryptic purine transporters in *Aspergillus nidulans* reveal the role of specific residues in the evolution of specificity in the NCS1 family. *Mol. Microbiol.* 103(2): 319–332.
- Stark, M.J. 1987. Multicopy expression vectors carrying the lac repressor gene for regulated high-level expression of genes in *Escherichia coli*. *Gene* 51(2-3): 255–267.
- Suzuki, S. and Henderson, P.J. 2006. The hydantoin transport protein from *Microbacterium liquefaciens*. *J. Bacteriol.* 188(9): 3329–3336.
- Szakonyi, G., Leng, D., Ma, P., Bettaney, K.E., Saidijam, M., Ward, A., Zibaei, S., Gardiner, A.T., Cogdell, R.J., Butaye, P., Kolsto, A.B., O'Reilly, J., Hope, R.J., Rutherford, N.G., Hoyle, C.J. and Henderson, P.J. 2007. A genomic strategy for cloning, expressing and purifying efflux proteins of the major facilitator superfamily. *J. Antimicrob. Chemother.* 59(6): 1265–1270.
- Timmis, K.N. 2002. *Pseudomonas putida*: a cosmopolitan opportunist par excellence. *Env. Microbiol.* 4(12): 779–781.
- Tsirigos, K.D., Peters, C., Shu, N., Käll, L. and Elofsson, A. 2015. The TOPCONS web server for consensus prediction of membrane protein topology and signal peptides. *Nucleic Acids Res.* 43(W1): W401–W407.
- Walsh, U.F., Morrissey, J.P. and O'Gara, F. 2001. *Pseudomonas* for biocontrol of phytopathogens: from functional genomics to commercial exploitation. *Curr. Opin. Biotechnol.* 12(3): 289–295.
- Ward, A., O'Reilly, J., Rutherford, N.G., Ferguson, S.M., Hoyle, C.K., Palmer, S.L., Clough, J.L., Venter, H., Xie, H., Litherland, G.J., Martin, G.E., Wood, J.M., Roberts, P.E., Groves, M.A., Liang, W.J., Steel, A., McKeown, B.J. and Henderson, P.J. 1999. Expression of prokaryotic membrane transport proteins in *Escherichia coli*. *Biochem. Soc. Trans.* 27(6): 893–899.
- Ward, A., Sanderson, N.M., O'Reilly, J., Rutherford, N.G., Poolman, B. and Henderson, P.J.F. 2000. The amplified expression, identification, purification, assay and properties of hexahistidine tagged bacterial membrane transport proteins. In: Baldwin SA (ed) *Membrane transport – a Practical Approach*, Oxford: Blackwell; p. 141–166.
- Weyand, S., Ma, P., Saidijam, M., Baldwin, J., Beckstein, O., Jackson, S., Suzuki, S., Patching, S.G., Shimamura, T., Sansom, M.S.P., Iwata, S., Cameron, A.D., Baldwin, S.A. and Henderson, P.J.F. 2010. The Nucleobase-Cation-Symport-1 family of membrane transport proteins (Chapter 11). In: *Handbook of Metalloproteins*. John Wiley and Sons. DOI: 10.1002/0470028637.met268
- Weyand, S., Shimamura, T., Beckstein, O., Sansom, M.S., Iwata, S., Henderson, P.J., and Cameron, A.D. 2011. The alternating access mechanism of transport as observed in the sodium-hydantoin transporter Mhp1. *J. Synchrotron. Radiat.* 18(1): 20–23.
- Weyand, S., Shimamura, T., Yajima, S., Suzuki, S., Mirza, O., Krusong, K., Carpenter, E.P., Rutherford, N.G., Hadden, J.M., O'Reilly, J., Ma, P., Saidijam, M., Patching, S.G., Hope, R.J., Norbertczak, H.T., Roach, P.C., Iwata, S., Henderson, P.J. and Cameron, A.D. 2008. Structure and molecular mechanism of a nucleobase-cation-symport-1 family transporter. *Science* 322(5902): 709–713.
- Winsor, G.L., Griffiths, E.J., Lo, R., Dhillon, B.K., Shay, J.A. and Brinkman, F.S. 2016. Enhanced annotations and features for comparing thousands of *Pseudomonas* genomes in the *Pseudomonas* genome database. *Nucleic Acids Res.* 44(D1): D646–D653.

Witholt, B., Boekhout, M., Brock, M., Kingma, J., Heerikhuizen, H.V. and Leij, L.D. 1976. An efficient and reproducible procedure for the formation of spheroplasts from variously grown *Escherichia coli*. Anal. Biochem. 74(1): 160–170.

Witz, S., Panwar, P., Schober, M., Deppe, J., Pasha, F.A., Lemieux, M.J. and

Möhlmann, T. 2014. Structure-function relationship of a plant NCS1 member--homology modeling and mutagenesis identified residues critical for substrate specificity of PLUTO, a nucleobase transporter from Arabidopsis. PLoS One 9(3): e91343.

Supplementary Information

(Supplementary Materials and Methods, Supplementary Tables S1-S2, Figures S1-S9)

Supplementary Materials and Methods

General

Chemicals, reagents and media of the highest available quality were obtained from Sigma-Aldrich Co., Fisher Scientific UK Ltd, Melford Laboratories Ltd, BDH Chemical Supplies or Difco Laboratories, unless stated otherwise. All media, buffers and other solutions were prepared using either deionised water or MilliQ™ water. All media were sterilised by autoclaving or for thermally-sensitive solutions by passage through 0.2 µM Minisart® high-flow sterile syringe-driven filters (Sartorius) or using vacuum-driven 0.2 µM filters (Stericup®) from Millipore. Cellulose nitrate 25 mm ø filters (0.45 µM pore size) for radiolabelled substrate assays and cellulose ester GSTF 25 mm ø filters (0.22 µM pore size) (Whatman®) for protein determinations were from Millipore (UK) Ltd. DNA purification kits were from QIAGEN Ltd. Restriction endonucleases and T4 DNA ligase were from New England Biolabs, Pfu Turbo™ DNA polymerase was from Agilent Technologies UK, and 1 kb DNA ladder and SYBR Safe™ DNA gel stain was from Invitrogen. PCR amplification of DNA was performed using a Peltier Thermal cycler from MJ Research. Cell disruption was performed using a Constant Systems disruptor. Protein determinations used the method of Schaffner and Weissmann (1973) or a BCA assay using Pierce® BCA protein assay reagent A from Thermo Scientific. SDS-PAGE was performed by the

method of Laemmli (1970), refined for membrane proteins as described by Henderson and Macpherson (1986) using 4% stacking gels and 15% resolving gels in a BioRad Mini PROTEAN 3 apparatus. Acrylamide (40%) and bisacrylamide (2%) solutions were from BioRad Laboratories and SDS-7 protein molecular weight markers were from Sigma-Aldrich Co. Western blotting was performed by semi-dry transfer using a BioRad TRANS-BLOT® SD apparatus; RGS-His₆ antibody was from QIAGEN Ltd, SuperSignal® West Pico luminal enhancer solution and stable peroxide solution were from Perbio Science UK and Fluorotrans™ membrane was from Pall BioSupport, UK. High-range Rainbow molecular weight markers were from Amersham Biosciences UK Ltd.

Gene cloning and transformation of *E. coli*

Cloning was performed using the plasmid pTTQ18 (Stark 1987), which is based on the pUC high expression series of plasmids with a polylinker/lacZ region flanked by the strong hybrid trp-lac (tac) promoter, which was later modified to introduce an RGS(His₆) tag at the C-terminal end of the protein (Ward et al. 1999; Ward et al. 2000). The strategy is outlined below. PCR primers were designed to extract and amplify the specific gene from genomic DNA of the relevant organism with introduction of *Eco*R1 and *Pst*I restriction sites at the 5' and 3' ends,

respectively, followed by digestion of the PCR product with these enzymes. The gene digests were ligated into the multi-cloning site of *EcoRI/PstI*-digested plasmid pTTQ18 downstream from the IPTG-inducible tac promoter and immediately upstream from a RGS(His₆)-coding sequence that we had already engineered into the plasmid (Liang, 1994, unpublished). The ligation product was transformed into *E. coli* Omnimax cells (Stratagene™) in the presence of carbenicillin (100 µg/ml) followed by PCR screening of colonies, extraction of plasmid DNA from positive clones and restriction digestion analysis using *EcoRI* and *PstI* enzymes. Plasmid DNA from successful ligations was transformed into *E. coli* BL21(DE3) cells (Novagen™) followed by a test for inducible expression of the His-tagged protein by SDS-PAGE and Western blot analysis of membranes prepared by the water lysis method (Witholt et al. 1976; Ward et al. 2000) from small-scale (50 ml) cell cultures that were uninduced or induced with IPTG (0.5 mM). Clones of cells that showed successful amplified expression of the proteins were transferred into a freezing mixture (12.6 g/L K₂HPO₄, 0.9 g/L sodium citrate, 0.18 g/L MgSO₄, 1.8 g/L (NH₄)₂SO₄, 3.6 g/L KH₂PO₄, 96 g/L glycerol), frozen in liquid nitrogen and stored at -80 °C. Competent cells were prepared by the methods described by Inoue et al. (1990) or Chung et al. (1989) and transformations were performed based on the method described by Inoue et al. (1990). For those proteins that showed some amplified expression, this was optimised by using ranges in the concentration of IPTG for induction (0-1 mM) and the length of induction (2-5 hours) and using three different types of media for cell growth (LB, 2TY, M9 minimal).

Cell growth and membrane preparation

Cells were grown in LB or 2TY liquid medium supplemented with glycerol (20 mM) and

carbenicillin (100 µg/ml) in Falcon tubes (10 ml in 50 ml tubes) for starter cultures and in LB, 2TY or M9 minimal medium in baffled flasks (50 ml in 250 ml flasks or 500 ml in 2 litre flasks for small-scale and large-scale cultures, respectively) at a temperature of 37 °C with shaking at 200 rpm. Cells were recovered from deep frozen stocks by streaking onto LB-agar plates with 100 µg/ml carbenicillin, using a single colony to inoculate LB medium in Falcon tubes, and then using a 2% (v/v) inoculum when transferring from one liquid culture to another. For expression tests and optimisation of induction conditions, small-scale cultures were grown to an A₆₀₀ of 0.4-0.6, then left uninduced or induced with the relevant concentration of IPTG and grown for the given further length of time before harvesting by centrifugation (3000 x g, 10 min, in Falcon tubes using a bench-top instrument), followed by preparation of membranes by the water lysis method (Witholt et al. 1976; Ward et al. 2000). For large-scale membrane preparation, typically a total of 10 litres of cells were grown to an A₆₀₀ of 0.4-0.6, then induced with IPTG (0.5 mM) and grown for a further 3 hours before harvesting by centrifugation (6000 x g, 15 min, 4 °C) and storage at -80 °C. At a later time the cells were thawed, suspended in Tris-EDTA buffer (20 mM Tris, pH 7.5 with 0.5 mM EDTA) and disrupted by passing twice through a cell disrupter (Constant Systems) at 30 kpsi. Undisrupted cells and cell debris were removed by centrifugation at 12000 x g for 45 minutes at 4 °C. The supernatant containing total (inner plus outer) membranes was collected and retained. Inner/outer membranes were separated by sucrose gradient ultracentrifugation and prepared as described in Ward et al. (2000), followed by washing and resuspension in Tris buffer (20 mM, pH 7.5), dispensing into aliquots, rapid freezing in liquid nitrogen and storage at -80 °C.

Supplementary Tables and Figures**Table S1.** Composition of buffers for protein solubilisation and purification.

	Tris-HCl	Glycerol	NaCl	SDS	Imidazole
Solubilisation buffer	20 mM (pH 8.0)	20% (v/v)	300 mM	1% (w/v)	20 mM
Wash buffer 1	10 mM (pH 8.0)	10% (v/v)	-	0.05% (w/v)	20 mM
Elution buffer	10 mM (pH 8.0)	2.5% (v/v)	-	0.05% (w/v)	200 mM
Wash buffer 2	10 mM (pH 7.6)	2.5% (v/v)	-	0.05% (w/v)	-

Table S2. Composition of buffers for fluorescence spectroscopy.

Stock solution	A. No added Na⁺		B. With added Na⁺	
	Final concentratio	Volum e	Final concentratio	Volum e
Choline chloride (1 M)	140 mM	700 μ l	125 mM	625 μ l
Tris (1 M, pH 7.5)	10 mM	50 μ l	10 mM	50 μ l
DDM (10% w/v)	0.05% (w/v)	25 μ l	0.05% (w/v)	25 μ l
DMSO	2% (v/v)	100 μ l	2% (v/v)	100 μ l
NaCl (4 M)	-	-	15 mM	18.75 μ l
MilliQ water	-	4.125 ml	-	4.181 ml
	Total	5 ml	Total	5 ml

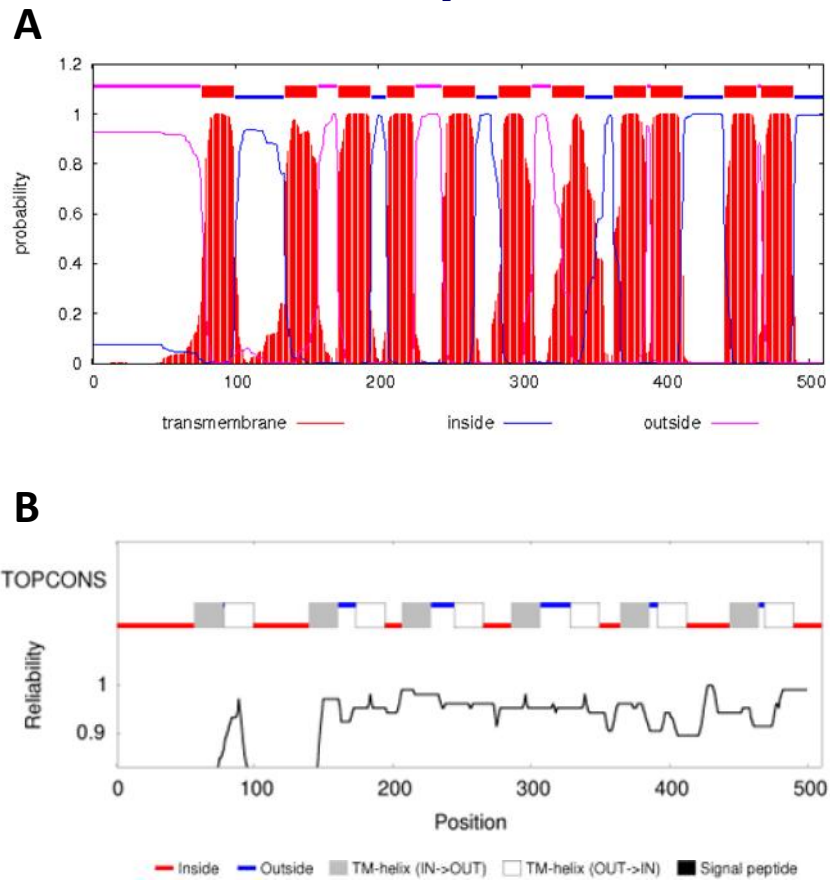


Figure S1. Predictions of transmembrane helices in *P. putida* protein AAN69889. The amino acid sequence of AAN69889 was taken from the UniProtKnowledgeBase (<http://www.uniprot.org/>) and analysed by the membrane topology prediction tools TMHMM (<http://www.cbs.dtu.dk/services/TMHMM/>) (Krogh et al. 2001) (A) and TOPCONS (<http://topcons.cbr.su.se/>) (Bernsel et al. 2009) (B).

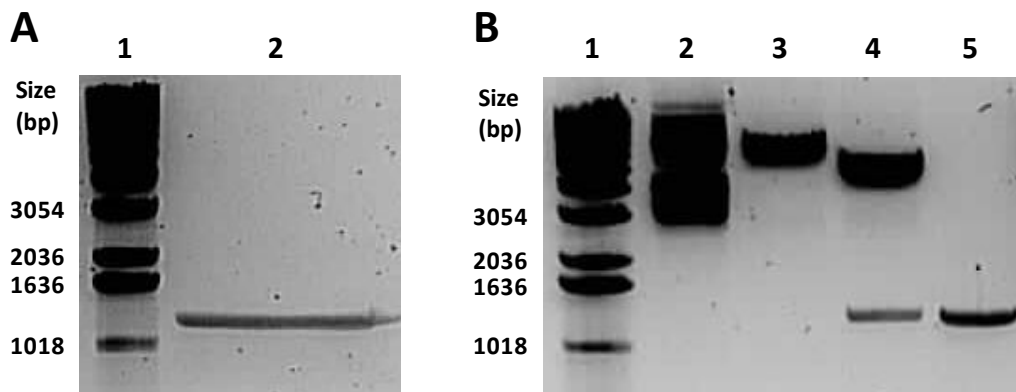


Figure S2. PCR amplification of the gene for *P. putida* protein AAN69889 and cloning into plasmid pTTQ18. Analysis on 1% agarose gels of **A**. The PCR product for amplifying the gene of *P. putida* protein AAN69889 (1 = DNA base pairs ladder, 2 = PCR product) and **B**. Restriction digestion of the plasmid construct for amplifying expression of *P. putida* protein AAN69889 (1 = DNA base pairs ladder, 2 = undigested plasmid, 3 = *EcoRI*-digested plasmid, 4 = *EcoRI/PstI*-digested plasmid, 5 = *EcoRI/PstI*-digested PCR product).

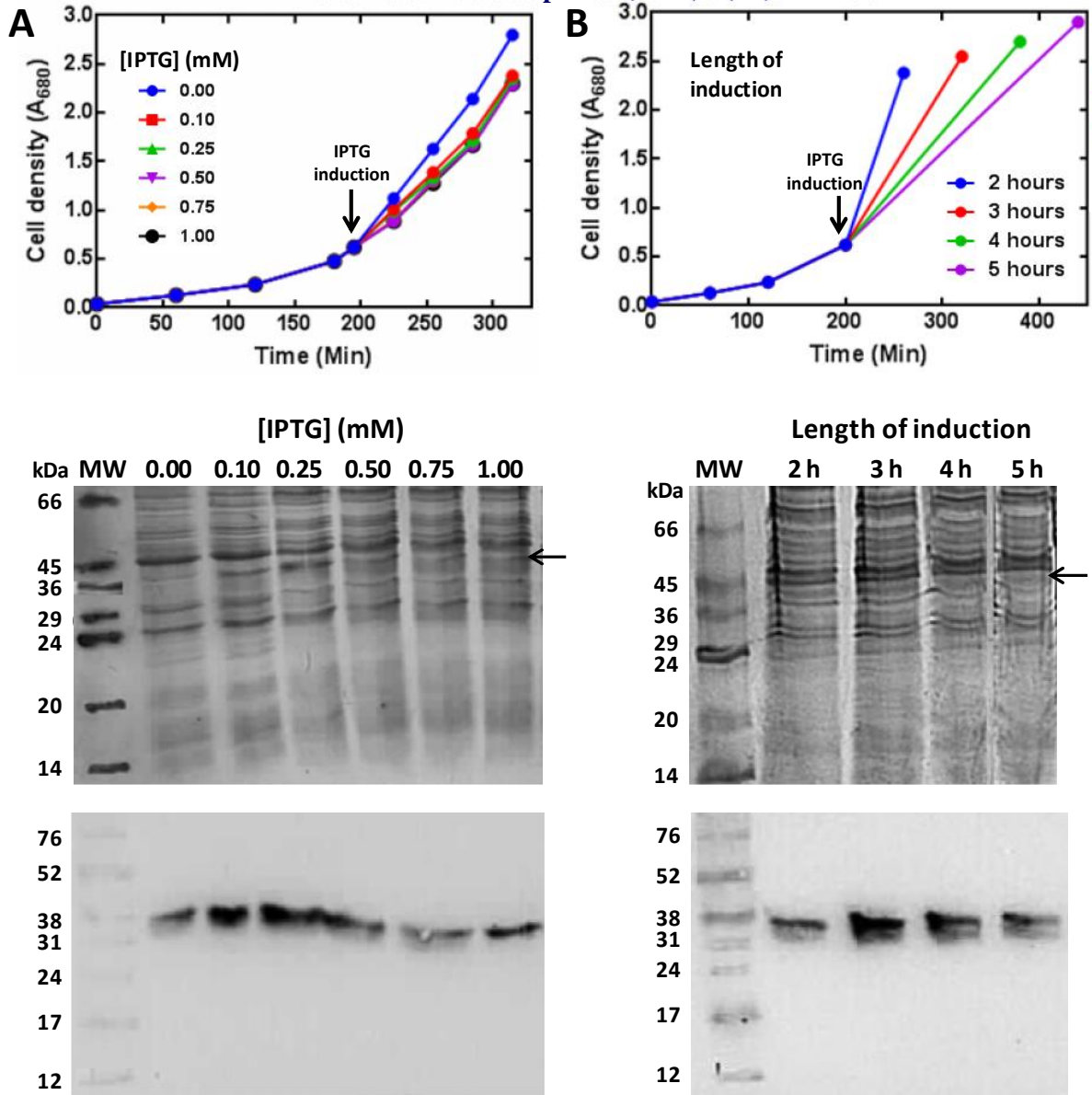


Figure S3. Optimisation of induction conditions for amplifying expression of *P. putida* protein AAN69889 in *E. coli*. Optimisation of IPTG concentration (**A**) and length of induction (**B**) for amplifying expression of AAN69889-His₆ in *E. coli* BL21 (DE3) cells using LB medium supplemented with glycerol (20 mM). Cells (50 ml) were grown in 250-ml flasks at a temperature of 37 °C with shaking at 220 rpm and induced at an A_{680} of ~0.6 using a range of concentrations of IPTG (A) or 0.25 mM IPTG (B). Growth curves (*top*), Coomassie-stained SDS-PAGE (*middle*) and Western blot (*bottom*) analyses of total membranes prepared are shown for each variable. MW = molecular weight markers, arrow = position of AAN69889-His₆.

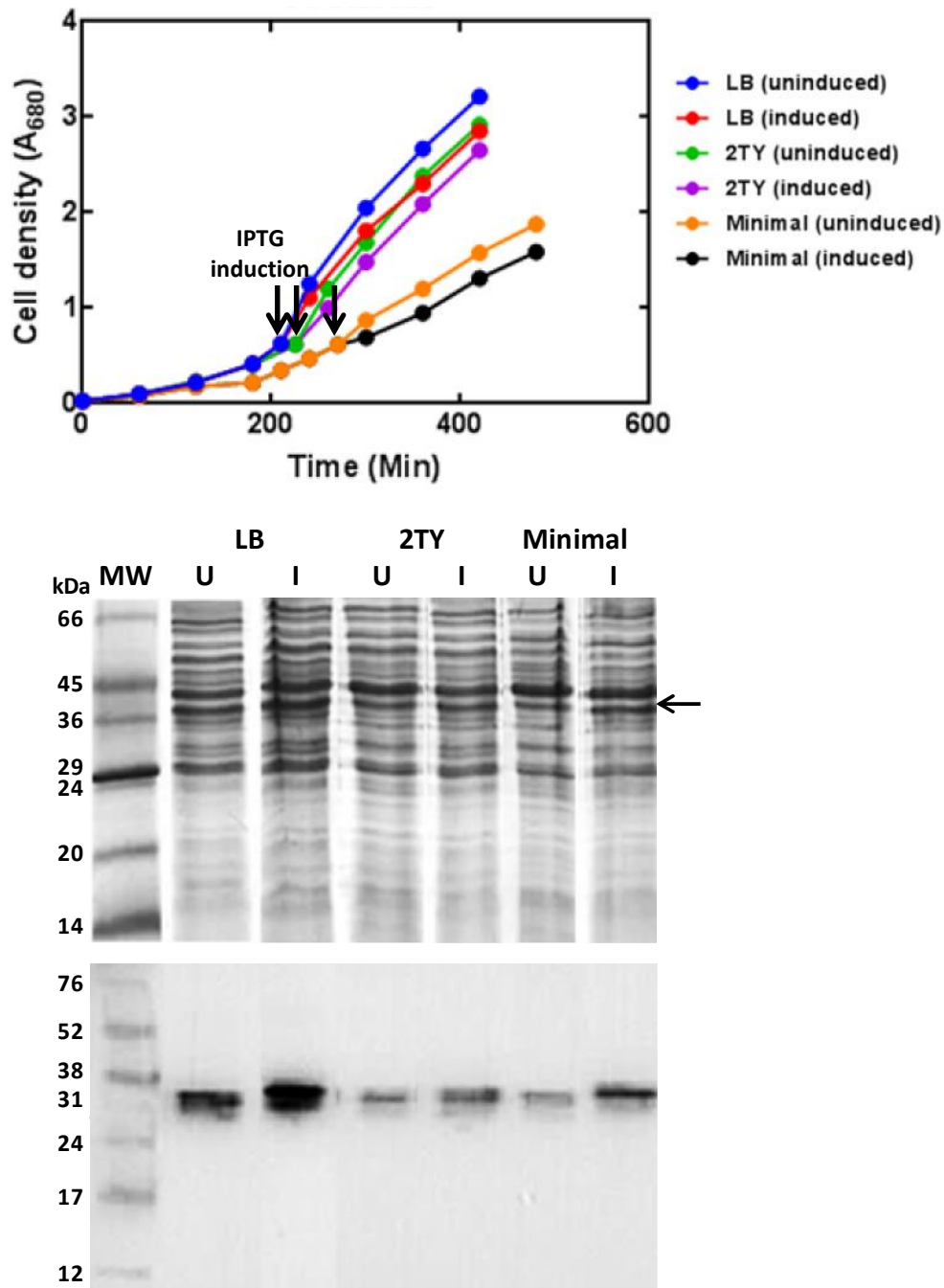


Figure S4. Optimisation of growth medium for amplifying expression of *P. putida* protein AAN69889 in *E. coli*. Growth curves (*top*), Coomassie-stained SDS-PAGE (*middle*) and Western blot (*bottom*) analyses of total membranes from *E. coli* BL21(DE3) cells harbouring the plasmid for amplifying expression of AAN69889-His₆ grown in different types of medium (LB, 2TY, M9 minimal) supplemented with glycerol (20 mM). Cells (50 ml) were grown in 250-ml flasks at 37 °C with shaking at 220 rpm and induced at an A_{680} of ~0.6 with IPTG (0.25 mM) for 3 hours. MW = molecular weight markers, U = uninduced, I = induced, arrow = position of AAN69889-His₆.

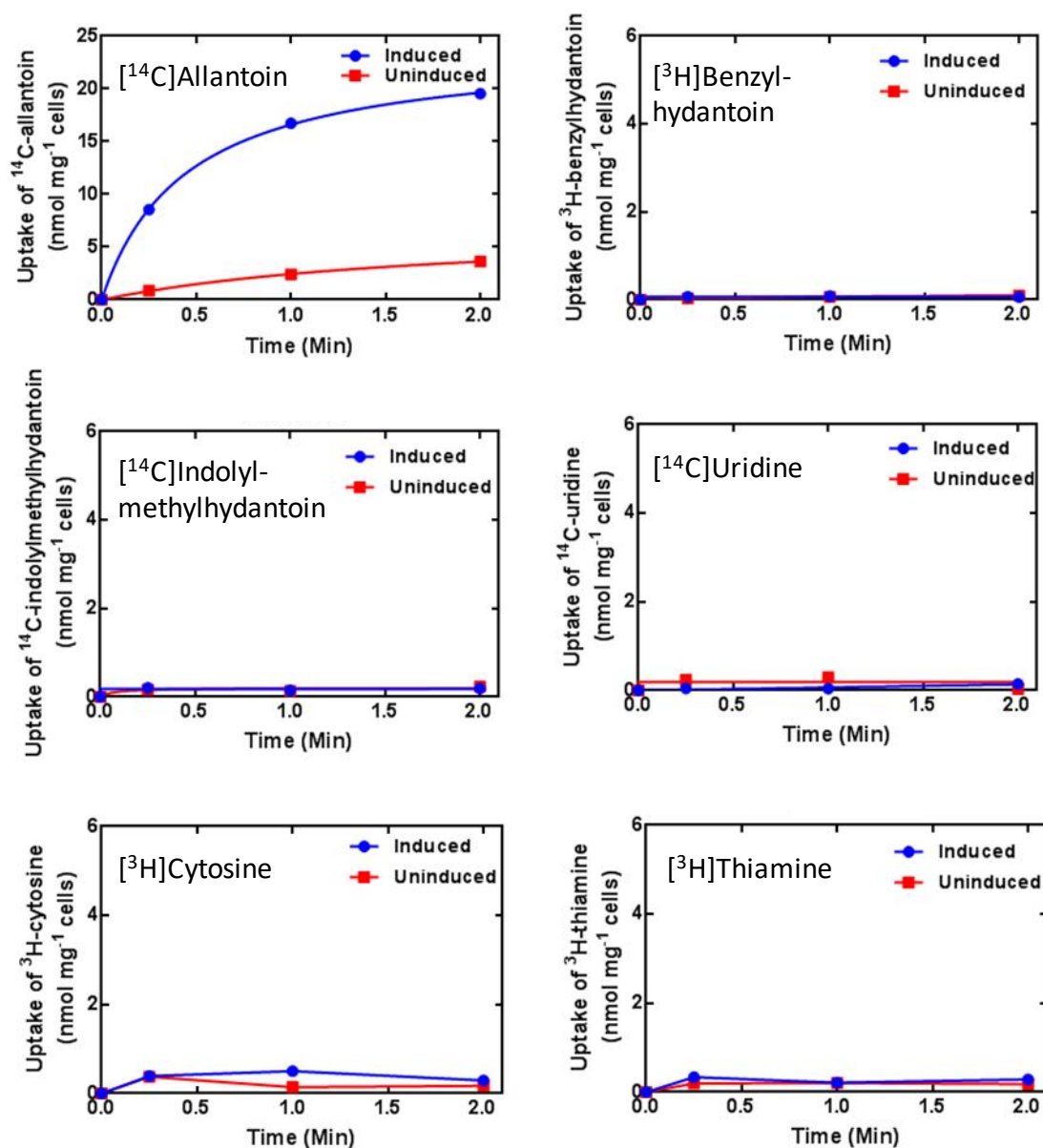


Figure S5. Possible transport of radiolabelled substrates by *P. putida* protein AAN69889. Uptake of potential radiolabelled substrates (50 μ M) into *E. coli* BL21(DE3) cells harbouring the plasmid pTTQ18/AAN69889. Cells were grown in LB medium supplemented with glycerol (20 mM) and of carbenicillin (100 μ g/ml) at 37 $^{\circ}$ C with shaking at 220 rpm. Cells were left uninduced (*red*) or were induced (*blue*) at $A_{680} = 0.6$ with IPTG (0.25 mM) and then grown for a further 1 hour. Harvested cells were washed three times using transport assay buffer (150 mM KCl, 5 mM MES pH 6.6) and resuspended in the same buffer to an accurate A_{680} of around 2.0. Cells were energised with glycerol (20 mM) and tested for uptake of the given potential radiolabelled substrates.

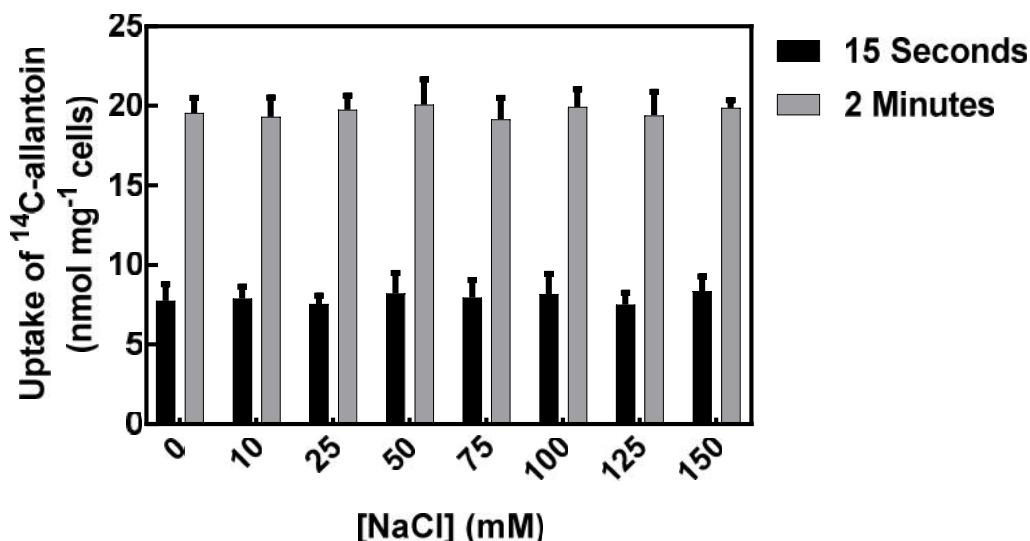


Figure S6. Effect of sodium ion concentration on uptake of ¹⁴C-allantoin by *P. putida* protein AAN69889. *E. coli* BL21 (DE3) cells harbouring the plasmid pTTQ18/AAN69889 were grown in LB medium supplemented with glycerol (20 mM) and carbenicillin (100 µg/ml) at 37 °C with shaking at 220 rpm. Cells were induced at A₆₈₀ = 0.6 with IPTG (0.25 mM) and then grown for a further 1 hour. Harvested cells were washed three times using transport assay buffer containing 5 mM MES (pH 6.6) and a range of NaCl concentrations from 0-150 mM, balanced by a range of KCl concentrations to maintain an overall salt concentration of 150 mM. Under conditions of zero NaCl, crown ether at a concentration of 10 mM was included to mop up any traces of NaCl. Cells were resuspended in the same buffer to an accurate A₆₈₀ of around 2.0. Aliquots of cells were energised with glycerol (20 mM) and tested for uptake of ¹⁴C-allantoin (50 µM) at the given time points. Data represent the average of duplicate measurements.

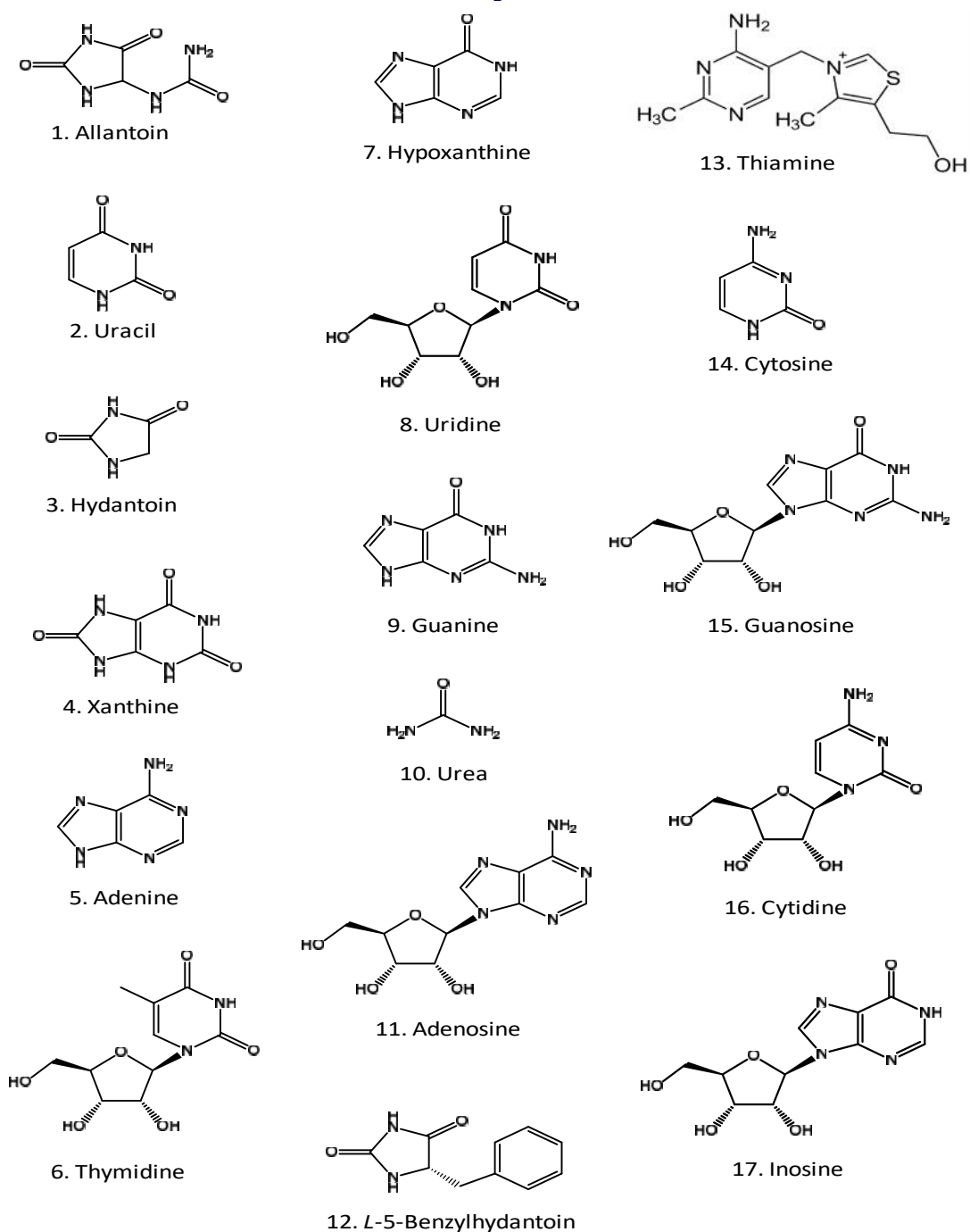


Figure S7. Structures of compounds used as potential competitors of AAN69889-mediated ^{14}C -allantoin uptake into whole cells. Structures 1-17 are arranged in order of decreasing competitive effect on AAN69889-mediated ^{14}C -allantoin uptake as shown in Figure 5 (main paper).

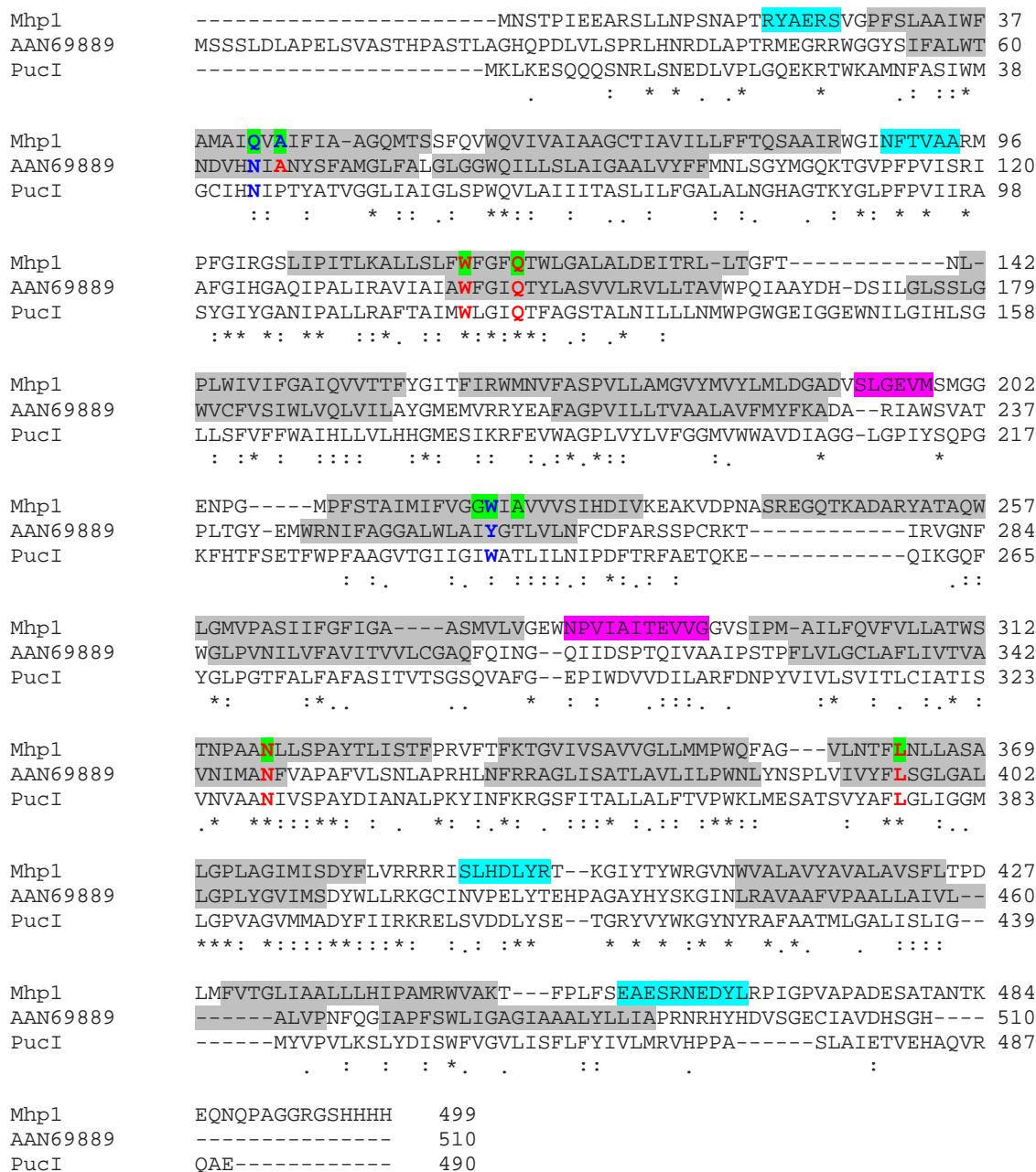


Figure S8. Conservation of residues between *P. putida* protein AAN69889, Mhp1 and PucI. Amino acid sequences of AAN69889 from *P. putida* (Q88EZ1), Mhp1 from *M. liquefaciens* (D6R8X8) and PucI from *B. subtilis* (P94575) were taken from the UniProtKnowledgeBase (<http://www.uniprot.org/>) and aligned using Clustal Omega (<http://www.ebi.ac.uk/Tools/msa/clustalo/>) (Sievers et al. 2011). Conserved residues are indicated below the sequences as identical (*), highly similar (:), and similar (.). Residues in the substrate binding site of Mhp1 are highlighted (green) and residues at these positions are coloured for those that are identical (red) or highly similar (blue) in the three proteins. Helical regions in Mhp1 based on the crystal structure of Mhp1 with bound benzylhydantoin (PDB 4D1B) (Simmons et al. 2014) are highlighted as follows: transmembrane helix (grey), internal helix (cyan), external helix (pink). Putative transmembrane helices in PucI based on TOPCONS prediction are also highlighted (grey).

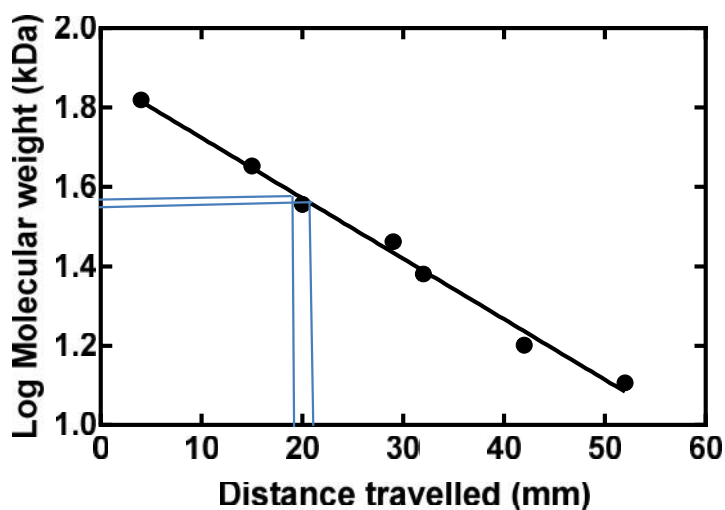



Figure S9. Estimation of AAN69889-His₆ molecular weight on an SDS-PAGE gel. Calibration graph for the distance travelled by AAN69889-His₆ protein bands on a Coomassie-stained SDS-PAGE gel (Figure 6 of main paper) based on migration of marker proteins of known molecular weight. The blue lines represent the distance travelled by AAN69889-His₆, which equate to molecular weights of 37 kDa and 38 kDa.

References

- Bernsel, A., Viklund, H., Hennerdal, A. and Elofsson, A. 2009. TOPCONS: consensus prediction of membrane protein topology. *Nucleic Acids Res.* 37 (Web Server issue): W465–W468.
- Chung, C.T., Niemela, S.L. and Miller, R.H. 1989. One-step preparation of competent *Escherichia coli*: transformation and storage of bacterial cells in the same solution. *Proc. Natl. Acad. Sci. U. S. A.* 86(7):2172–2175.
- Henderson, P.J., and Macpherson, A.J. 1986. Assay, genetics, proteins, and reconstitution of proton-linked galactose, arabinose, and xylose transport systems of *Escherichia coli*. *Methods Enzymol.* 125:387–429.
- Inoue, H., Nojima, H. and Okayama, H. 1990. High efficiency transformation of *Escherichia coli* with plasmids. *Gene* 96 (1):23–28.
- Krogh, A., Larsson, B., von Heijne, G. and Sonnhammer, E.L. 2001. Predicting transmembrane protein topology with a hidden Markov model: application to complete genomes. *J. Mol. Biol.* 305(3):567–580.
- Laemmli, U.K. 1970. Cleavage of structural proteins during the assembly of the head of bacteriophage T4. *Nature* 227 (5259): 680–685.
- Schaffner, W. and Weissmann, C. 1973. A rapid, sensitive, and specific method for the determination of protein in dilute solution. *Anal. Biochem.* 56(2):502–514.
- Sievers, F., Wilm, A., Dineen, D., Gibson, T.J., Karplus, K., Li, W., Lopez, R., McWilliam, H., Remmert, M., Söding, J., et al. 2011. Fast, scalable generation of high-quality protein multiple sequence alignments using Clustal Omega. *Mol. Syst. Biol.* 7:539.
- Simmons, K.J., Jackson, S.M., Brueckner, F., Patching, S.G., Beckstein, O., Ivanova, E., Geng, T., Weyand, S., Drew, D., Lanigan, J., et al. 2014. Molecular mechanism of ligand recognition by membrane transport protein, Mhp1. *EMBO J.* 33(16): 1831–1844.

- Stark, M.J.1987.Multicopy expression vectors carrying the lac repressor gene for regulated high-level expression of genes in *Escherichia coli*.*Gene* 51 (2-3):255–267.
- Ward, A., O'Reilly, J., Rutherford, N.G., Ferguson, S.M., Hoyle, C.K., Palmer, S.L., Clough, J.L., Venter, H., Xie, H., Litherland, G.J.et al. 1999.Expression of prokaryotic membrane transport proteins in *Escherichia coli*. *Biochem. Soc. Trans.*27(6):893–899.
- Ward, A., Sanderson, N.M., O'Reilly, J., Rutherford, N.G., Poolman,B. and Henderson, P.J.F.2000.The amplified expression, identification, purification, assay and properties of hexahistidine tagged bacterial membrane transport proteins. In: Baldwin SA (ed) *Membrane transport – a Practical Approach*. Blackwell, Oxford, pp 141–166.
- Witholt, B., Boekhout, M., Brock, M., Kingma, J., Heerikhuizen, H.V. and Leij, L.D.1976.An efficient and reproducible procedure for the formation of spheroplasts from variously grown *Escherichia coli*. *Anal.Biochem.*74(1):160–170.

Access this Article in Online	
	Website: www.ijarm.com
	Subject: Molecular Biology
Quick Response Code	
DOI: 10.22192/ijamr.2022.09.12.011	

How to cite this article:

Irshad Ahmad, Karl A. Hassan, Peter J. F. Henderson and Simon G. Patching. (2022). Cloning, Amplified Expression, Functional Characterisation and Purification of a *Pseudomonas putida* NCS1 Family Transport Protein. *Int. J. Adv. Multidiscip. Res.* 9(12): 127-156.
DOI: <http://dx.doi.org/10.22192/ijamr.2022.09.12.011>